



LUND UNIVERSITY

Numerical Studies of Methanol PPC Engines and Diesel Sprays

Pucilowski, Mateusz

2019

Document Version:

Publisher's PDF, also known as Version of record

[Link to publication](#)

Citation for published version (APA):

Pucilowski, M. (2019). *Numerical Studies of Methanol PPC Engines and Diesel Sprays*. Energy Sciences, Lund University.

Total number of authors:

1

General rights

Unless other specific re-use rights are stated the following general rights apply:

Copyright and moral rights for the publications made accessible in the public portal are retained by the authors and/or other copyright owners and it is a condition of accessing publications that users recognise and abide by the legal requirements associated with these rights.

- Users may download and print one copy of any publication from the public portal for the purpose of private study or research.
- You may not further distribute the material or use it for any profit-making activity or commercial gain
- You may freely distribute the URL identifying the publication in the public portal

Read more about Creative commons licenses: <https://creativecommons.org/licenses/>

Take down policy

If you believe that this document breaches copyright please contact us providing details, and we will remove access to the work immediately and investigate your claim.

LUND UNIVERSITY

PO Box 117
221 00 Lund
+46 46-222 00 00

Numerical Studies of Methanol PPC Engines and Diesel Sprays

Numerical Studies of Methanol PPC Engines and Diesel Sprays

by Mateusz Pucilowski



LUND
UNIVERSITY


Thesis for the degree of Philosophy in Engineering
Thesis advisors: Prof. Xue-Song Bai, Dr. Mehdi Jangi
and Assistant Prof. Hesameddin Fatehi
Faculty opponent: Assoc. Prof. Bart Somers

To be presented, with the permission of the Faculty of Engineering of Lund University, for public criticism in the lecture hall M:B, M-building, at the Department of Energy Sciences on the 29th of November 2019 at

10:15.

Organization LUND UNIVERSITY Department of Energy Sciences Box 118 SE-221 00 LUND Sweden		Document name DOCTORAL DISSERTATION	
		Date of disputation 2019-11-29	
		Sponsoring organization MOT-2030, Competence Center for Combustion Processes KCFP	
Author(s) Mateusz Pucilowski			
Title and subtitle Numerical Studies of Methanol PPC Engines and Diesel Sprays			
Abstract <p>The global environment suffers from utilizing fossil fuels to powering internal combustion engines (ICE), due to the massive amounts of released CO₂. Besides the global impact, the local environments experience high concentrations of harmful pollutants such as NO_x, CO, soot and particulate matter (PM). The automotive industry is continuously striving to find new solutions to decrease the fuel consumption and also to develop cleaner and more advanced combustion systems, i.e., low temperature combustion (LTC) engines.</p> <p>The goal of this thesis is to employ computational fluid dynamics (CFD) simulations to investigate methanol under the partially premixed combustion (PPC) regime, which is one of the advanced LTC concepts alongside HCCI and RCCL. The benefit of PPC engines is the reduced average combustion temperature, which results in optimized emission rates of UHC/CO and NO_x, maintaining a high thermal efficiency. Interesting properties of methanol, such as a low stoichiometric air to fuel ratio and a high latent heat of vaporization as well as non-sooting combustion, may enable further improvement of the PPC concept. Studies have been carried out by employing RANS and LES models to simulate mixing and ignition processes. It was found that methanol PPC can be achieved at relatively later injection timings (similar to those in diesel engines), in comparison to gasoline. Late injection timings can ease injection targeting into the piston bowl and utilize strong wall-spray interaction to help control the in-cylinder flow and therefore reduce the wall heat losses. The well-stirred-reactor (WSR) approach fails to predict pressure traces at highly stratified mixture compositions, such as $0.3 < \phi < 2.5$. Instead, the partially-stirred-reactor (PaSR) model, after model constant calibration, was employed to improve the prediction of combustion behavior. The ignition kernel of methanol starts in the fuel leanest mixtures, and continues as an ignition front propagation towards the fuel rich mixtures, consuming the remaining fuel that has originated from the fuel rich side, in the diffusion flame mode.</p> <p>In the second part of the thesis focus is set on the diesel spray - wall interaction. LES is employed to study the air entrainment mechanisms, such as flame lift-off length, impingement mixing and entrainment wave, to identify their importance on the soot oxidation process. The free jet and wall impingement jets at 30 mm and 50 mm distance between the nozzle and the impingement wall are considered. The main finding is the non-monotonic mixing enhancement during combustion. The soot formation mixtures ($1600 K < T < 2200 K$, $\phi > 2$) can be accumulated in the near wall region, until the impingement vortices are developed, which then accelerates the mixing rate. Both wall jets resulted in more entrained air after the end on injection, which is considered to be the main reason for the faster oxidation of soot, with comparison to the free jet, which is in agreement with experimental measurements of the optical soot thickness KL.</p>			
Key words methanol, partially premixed combustion, PPC, spray-wall interaction, piston geometry, multiple injections, ICE, RANS, LES, ignition front, diffusion flame, combustion mode			
Classification system and/or index terms (if any)			
Supplementary bibliographical information		Language English	
ISSN and key title 0282-1990		ISBN 978-91-7895-318-9 (print) 978-91-7895-319-6 (pdf)	
Recipient's notes		Number of pages 168	Price
		Security classification	

I, the undersigned, being the copyright owner of the abstract of the above-mentioned dissertation, hereby grant to all reference sources the permission to publish and disseminate the abstract of the above-mentioned dissertation.

Signature 

Date 2019-10-30

Numerical Studies of Methanol PPC Engines and Diesel Sprays

by Mateusz Pucilowski



LUND
UNIVERSITY

Funding information: STEM MOT-2030 project with grant number 38272-1, and the Competence Center for Combustion Processes KCFP

Cover illustration: Rendering of temperature field at CAD 5 aTDC for LES study of double injection case with SOI -17/-3 aTDC.

© Mateusz Pucilowski 2019

Department of Energy Sciences
Faculty of Engineering
Lund University
Box 118
SE-221 00 LUND
Sweden

ISBN: 978-91-7895-318-9 (print)

ISBN: 978-91-7895-319-6 (pdf)

ISSN: 0282-1990

ISRN: LUTMDN/TMHP-19/1154-SE

Printed in Sweden by Tryckeriet i E-huset, Lund University, Lund 2019

Nothing in life is to be feared, it is only to be understood!
— Marie Curie-Sklodowska

Abstract

The global environment suffers from utilizing fossil fuels to powering internal combustion engines (ICE), due to the massive amounts of released CO_2 . Besides the global impact, the local environments experience high concentrations of harmful pollutants such as NO_x , CO , soot and particulate matter (PM). The automotive industry is continuously striving to find new solutions to decrease the fuel consumption and also to develop cleaner and more advanced combustion systems, i.e., low temperature combustion (LTC) engines.

The goal of this thesis is to employ computational fluid dynamics (CFD) simulations to investigate methanol under the partially premixed combustion (PPC) regime, which is one of the advanced LTC concepts alongside HCCI and RCCI. The benefit of PPC engines is the reduced average combustion temperature, which results in optimized emission rates of UHC/CO and NO_x , maintaining a high thermal efficiency. Interesting properties of methanol, such as a low stoichiometric air to fuel ratio and a high latent heat of vaporization as well as non-sooting combustion, may enable further improvement of the PPC concept. Studies have been carried out by employing RANS and LES models to simulate mixing and ignition processes.

It was found that methanol PPC can be achieved at relatively later injection timings (similar to those in diesel engines), in comparison to gasoline. Late injection timings can ease injection targeting into the piston bowl and utilize strong wall-spray interaction to help control the in-cylinder flow and therefore reduce the wall heat losses. The well-stirred-reactor (WSR) approach fails to predict pressure traces at highly stratified mixture compositions, such as $0.3 < \phi < 2.5$. Instead, the partially-stirred-reactor (PaSR) model, after model constant calibration, was employed to improve the prediction of combustion behavior. The ignition kernel of methanol starts in the fuel leanest mixtures, and continues as an ignition front propagation towards the fuel rich mixtures, consuming the remaining fuel that has originated from the fuel rich side, in the diffusion flame mode.

In the second part of the thesis focus is set on the diesel spray - wall interaction. LES is employed to study the air entrainment mechanisms, such as flame lift-off length, impingement mixing and entrainment wave, to identify their importance on the soot oxidation process. The free jet and wall impingement jets at 30 mm and 50 mm distance between the nozzle and the impingement wall are considered. The main finding is the non-monotonic mixing enhancement during combustion. The soot formation mixtures ($1600\text{K} < T < 2200\text{K}$, $\phi > 2$) can be accumulated in the near wall region, until the impingement vortices are developed, which then accelerates the mixing rate. Both wall jets resulted in more entrained air after the end on injection, which is considered to be the main reason for the faster oxidation of soot, with comparison to the free jet, which is in agreement with experimental measurements of the optical soot thickness KL.

Popularvetenskaplig sammanfattning

Numeriska modeller av förbränningsprocesser i bilmotorer spelar en viktig roll i den moderna utvecklingen av bilindustrin, som strävar efter lägre emissioner och bättre bränsleekonomi. Målet är att med hjälp av datorsimulationer skapa och utöka förståelsen för det turbulenta cylinderflödet och dess interaktion med flammor och kemiska reaktioner för att kunna styra och förbättra förbränningsprocessen.

Motorerna med högst verkningsgrad använder dieselcykeln, där förbränningen sker pga. kompressionen av den instängda luften, vilket ökar dess tryck och temperatur i förbränningskammaren. Bränslen som sprutas in direkt till förbränningskammaren när trycket och temperaturen är tillräckligt hög, evaporerar och antänds efter en kort tid. Insprutningen av bränsle fortsätter beroende på hur mycket arbete motorn ska leverera. Dieselcykeln karaktäriseras däremot med hög förbränningstemperatur som leder till höga emissioner av nitrid-oxider (NO_x) och av bränslerik förbränning som leder till höga sotemissioner. Båda visade sig vara väldigt farliga för människans hälsa, speciellt inom stora städer där emissioner når höga koncentrationer.

Under de två senaste årtiondena har forskning fokuserat på hur tidpunkten av bränslein-sprutning kan ändras för att utöka tiden för bränsleluftförblandning innan antändningen, vilket ska resultera i en lägre förbränningstemperatur och bränslemager förbränning och därför lägre emissioner. Sådan typ av förbränning kallas för delvis förblandad förbränning, eller på engelska "partially premixed combustion" (PPC). Problemet ligger i det komplexa och turbulenta flöde som uppstår när bränsle sprutas in och interagerar med väggarna i förbränningskammaren tidigt i komprimeringslaget. Beroende på distributionen av bränsleluftblandning och på hur långt motorkolven har kommit i komprimeringslaget, kommer antändningstidpunkten och hastigheten på reaktionsfronten att variera, vilket leder till svårigheter av kontrollerad repetition av förbränningen som en motor skall ha.

Denna avhandling fokuserar därför på datorsimulationer av bränsleinsprutnings processer för att kunna förutsäga var och när antändningen av bränsleluftblandningen kommer att ske i förbränningskammaren och i vilken takt reaktionsfronten kommer att propagera inom förbränningskammaren. Det har visat sig att termodynamiska egenskaper av metanol tillåter betydligt senare insprutningstider jämfört med konventionella bränsle som diesel eller bensen för att uppnå delvis förblandad förbränning. Däremot pga. stark kylningsförmåga av metanol vid insprutningen, måste motor ha ett högt kompressionsförhållande eller tillgång till en hög insugstemperatur för att uppnå en antändningsprocess. Simuleringarna har också visat att avancerade insprutningstrategier som inkluderar dubbla eller trippelinjektioner, kan sänka kravet på insugstemperatur. Utöver detta har olika geometrier på förbränningskammare studerats för att identifiera hur heta förbränningsprodukter rör sig inuti förbränningskammaren, vilket styr värmeförluster genom väggar.

I den andra delen av avhandlingen inkluderas simuleringar av dieselförbränning i ett konstant volymkärl med optisk tillgång där förbränningens parametrar kan isoleras och studeras individuellt. Utförd studie fokuserar på hur dieselflamman interagerar med en rak vägg beroende på avståndet från bränsleinsprutare. Olika avstånd ändrar turbulenta flödestrukturer nära väggen som styr hur snabbt luften kan blandas in i en dieselflamma, vilket leder till bättre oxidation av sotemissioner.

Acknowledgements

This work was carried out at the Department of Energy Sciences, Lund University, Sweden. The work was a part of STEM MOT2030 project and a part of KCFP Engine Research Center. Performed simulations were carried out on resources provided by the Swedish National Infrastructure for Computing (SNIC) at PDC and HPC2N.

I would like to give my deep gratitude to my main supervisor Prof. Xue-Song Bai for giving me the opportunity to work on this project. I am grateful for all discussions, all kindness, and all knowledge that I could ask for at any time. I would also like to express my gratitude to my co-supervisor Dr. Mehdi Jangi, for his mentoring and research inspiration. Mehdi had as much impact on me, as on my office computer, which led to totally random snapshots of Mehdi during the Skype meetings, that would suddenly pop-out on the screen, while discussing something with colleagues. I would also like to acknowledge my second co-supervisor, Assistant Prof. Hesameddin Fatehi. Thank you for all your help and giving lots of good and constructive criticisms, which I always got at the right moments.

I would like to give special thanks to my colleagues Christian, Hamed, Thommie, and Ali! Your impact on every day life at work was irreplaceable. All conversations, all laughs, all arguing, including some serious (scientific ones), made things interesting and worth to continue to work on. I also want to thank Johan, Rixin, Lei, Yaopeng, Senbin, Shijie, Michael, Morteza, Monika, Francesco and Mark for all created memories! Then, I would like to thank Dr. Robert Szasz and Prof. Johan Revstedt for improving my understanding on fluid mechanics and turbulence modeling throughout my time at LTH.

Here, I would like to thank to my chief engine researcher Dr. Sam Shamun. Thank You Sam, for the time I could share with you in the engine lab and for all data that was provided to perform CFD simulations. I want to even thank you twice, since the opportunity of doing Ph.D. about PPC engines came from you, and that piece of information was truly life changing, for which I am eternally grateful.

I would also like to thank Alexios and Sara for their effort for providing optical engine data for methanol combustion, which showed to be quite challenging. My colleagues at combustion engine department Changle Li, Amir, Nhut, Erik, Vikram, Niko, Nika and Ted, thank you for all your time and engine/car related discussions. I would also like to express my gratitude to combustion engine seniors Martin, Öivind, Sebastian and Per. Thank you for all discussions and sharing knowledge about engines (especially during traveling to conferences), and for the almost irresistible, kind and sharp sense of humor.

Most of all, I would like to thank to my parents and sister, Maciej, Izabella and Monika, and to my love Elin, for everything you have done to support me during this time!

List of publications

This thesis is based on the following publications, referred to by their Roman numerals:

- I **Effect of Start of Injection on the Combustion Characteristics in a Heavy-Duty DICl Engine Running on Methanol**
M. Pucilowski, Mehdi Jangi, Sam Shamun, Changle Li, Martin Tunér, Xue-Song Bai
SAE Technical Paper 2017-01-0560, 2017
- II **Effect of Injection Pressure on the NO_x Emission Rates in a Heavy-Duty DICl Engine Running on Methanol**
M. Pucilowski, Mehdi Jangi, Sam Shamun, Martin Tunér, Xue-Song Bai
SAE Technical Paper 2017-01-2194, 2017
- III **Heat Loss Analysis for Various Piston Geometries in a Heavy-Duty Methanol PPC Engine**
M. Pucilowski, Mehdi Jangi, Sam Shamun, Martin Tunér, Xue-Song Bai
SAE Technical Paper 2018-01-1726, 2018
- IV **Comparison of Kinetic Mechanisms for Numerical Simulation of Methanol Combustion in DICl Heavy-Duty Engine**
M. Pucilowski, Rui Li, Shijie Xu, Changle Li, Fei Qin Martin Tunér, Xue-Song Bai, Alexander A. Konnov
SAE Technical Paper 2018-01-0208, 2018
- V **Numerical Investigation of Methanol Ignition Sequence in an Optical PPC Engine with Multiply Injection Strategies**
M. Pucilowski, Hesameddin Fatehi, Mehdi Jangi, Sara Lönn, Alexios Matamis, Öivind Andersson, Mattias Richter, Xue-Song Bai
14th international Conference on Engines & Vehicles, 19ICENA-0262, 2019
- VI **LES study of diesel spray/wall interaction and mixing mechanisms at different wall distances**
M. Pucilowski, Mehdi Jangi, Hesameddin Fatehi, Kar Mun Pang, Xue-Song Bai
Preprint submitted to Proceedings of the Combustion Institute

Contents

Abstract	i
Popularvetenskaplig sammanfattning	iii
Acknowledgements	v
List of publications	vi
1 Introduction	1
1.1 Background	1
1.2 Thesis scope and objectives	2
1.3 Thesis contribution	3
1.4 Outline	4
2 Compression ignition engines	5
2.1 Combustion concept	5
2.2 Partially premixed combustion engines	8
2.2.1 Methanol as a PPC engine fuel	10
2.3 Ignition front wave, premixed flame, non-premixed flame	13
2.4 Mixing mechanisms in Diesel sprays	16
2.4.1 Impingement sprays	16
2.4.2 Multiple injection strategies	18
2.5 Development of combustion chamber	19
3 Governing equations of reactive flows	21
3.1 Turbulence	22
3.1.1 U-RANS formulation	24
3.1.2 LES formulation	25
3.2 Turbulent combustion scales	26
3.3 Mixture fraction and injection tracking	26
3.4 Spray modeling	27
3.5 Combustion models	28
3.6 Kinetics and speedup algorithms	30
3.7 Numerical solver	30
4 Methodology	31
4.1 Grid techniques	31

4.2	Boundary conditions	32
4.3	Heat release rate analysis	32
4.4	Experimental methods	32
4.4.1	Metal engine experiments	33
4.4.2	Optical engine experiments	33
4.4.3	Soot measurements	33
5	Results and discussion: methanol PPC engine	35
5.1	The role of start of injection	35
5.1.1	SOI sweep -20 to -3 at CR 15:1	35
5.1.2	SOI sweep -26 to -3 at CR 17.3:1	40
5.2	Effect of injection pressure on NO_x	43
5.3	Piston design study with focus on wall heat losses	45
5.4	Kinetic mechanisms	48
5.5	Combustion analysis of single and double injection strategy	50
5.6	Transient liquid penetration length	56
6	Results and discussion: diesel spray - wall interaction	59
6.1	Influence of wall position	59
7	Summary	67
7.1	Concluding remarks	67
7.2	Future work	69
	Bibliography	80
	Summary of publications	81
	Paper I: Effect of Start of Injection on the Combustion Characteristics in a Heavy-Duty DICI Engine Running on Methanol	85
	Paper II: Effect of Injection Pressure on the NO_x Emission Rates in a Heavy-Duty DICI Engine Running on Methanol	97
	Paper III: Heat Loss Analysis for Various Piston Geometries in a Heavy-Duty Methanol PPC Engine	107
	Paper IV: Comparison of Kinetic Mechanisms for Numerical Simulation of Methanol Combustion in DICI Heavy-Duty Engine	121
	Paper V: Numerical Investigation of Methanol Ignition Sequence in an Optical PPC Engine with Multiply Injection Strategies	135
	Paper VI: LES study of diesel spray/wall interaction and mixing mechanisms at different wall distances	151

Chapter 1

Introduction

1.1 Background

The transportation sector is constantly growing together with the world population, world economy and our living standard. The main power-train system driving cars, trucks and ferries is based on the internal combustion engine technology, where majority of energy demand is met by the fossil fuels. The drawback is a massive amount of released emissions of CO₂ and other harmful pollutants such as soot, nitride oxides NO_x and particular matter (PM). Emissions damage global and local environments, including our health and, therefore, the current condition of the transportation sector is not sustainable [1, 2].

Industry is continuously focusing on the development of cleaner power-train systems. Currently, electrification trends are in focus, where batteries are used as the energy carriers that drive the electrical motors installed in vehicles. The main benefit of electrification is the local zero emissions output, which can contribute to cleaner air in large urban areas. However, the green house gases, are still being released, but during the production of batteries and electricity at remote locations. Thereby, emission output is correlated with the source of electricity, which can be based on wind and solar power, but also on coal and natural gas. Thus, it is more beneficial to run electrical vehicles for example, in Nordic countries, compared to China or India. Moreover, due to the price and weight of electrical power-trains, the conversion of the entire ICE fleet today remains challenging [3, 4].

Other actions taken in order to reduce the impact of transportation sector on the environment are engine-hybrid solutions, platforms for shared vehicles and self-driving vehicles. All alternative transportation solutions are important in the global effort for better and sustainable transportation sector. However, due to the enormous size of the ICE fleet, it is expected that ICE will remain as a major power-train system, especially in the rural heavy-duty sector, where high energy density is essential. Hence, in order to reduce emissions of CO₂ and other pollutants released during the combustion process, the development of

ICE needs to continue.

The most common heavy-duty engine is based on the Diesel cycle, as it consumes less fuel compared to its gasoline rivals. Additionally diesel engines have better work characteristics suited to carry heavy loads. The challenge is the high emission output of NO_x , soot and particular matter (PM). In the modern diesel vehicles emissions formed inside of the combustion chamber are greatly reduced with help of the after-treatment systems as soot particle filters [5] and NO_x traps [6]. However, despite the after treatment systems which are also costly to maintain, new emission regulations as EURO VI continuously force engine manufacturers to further reduce emission output. Thus new technical solutions are required.

During the last two decades combustion engine research community was focused on the development of alternative combustion systems. Concepts such as homogeneous charge compression ignition (HCCI), reactivity controlled charge ignition (RCCI) and partially premixed combustion (PPC) were developed based on the low temperature combustion (LTC) concept, which results in cleaner emissions already in the combustion chamber. LTC engine concepts are promising and work excellent in the engine laboratory cell, however they barely exist on the global commercial scale due to the technical challenges regarding robustness of the combustion process, which is needed in the commercial applications [7, 8]. A number of different challenges are, for example, a limited operation load range due to the mechanical constraints, cold start issues or sensitivity to the inlet conditions. LTC engines are also characterized by a low exchange gas efficiency in comparison to Diesel engines, which can result in a similar brake thermal efficiency, despite an improved in-cylinder combustion process.

The combustion process in LTC engines is mainly driven by the fuel kinetics. Hence, properties and ignition mechanism of a specific fuel can have a significant effect on the engine performance. Different types of diesel and gasoline fuels were extensively investigated during the last decade. Recently focus was set on some alternative fuels as for example methanol. The properties of methanol are significantly different from diesel and gasoline, which potentially allows to improve some of the technical challenges.

1.2 Thesis scope and objectives

Modern development of combustion processes employs numerical modeling to gain in-depth understanding for the underlying mechanisms. The aim of thesis is to employ Computational Fluid Dynamics (CFD) simulations to investigate how unique properties of methanol, such as the low stoichiometric air to fuel ratio (A/F_s), and high latent heat of vaporization will affect the combustion characteristics and engine performance under partially premixed combustion regime. Simulations are used to study fuel injection, evolu-

tion of mixture composition, chemical kinetics and the spatial and temporal distribution of combustion reactions. Focus is set on understanding the underlying mechanisms governing the engine efficiency and emissions observed in the state-of-the-art experimental work on metal and optical engines employing laser diagnostics. Both turbulence modeling approaches as Large Eddy Simulation (LES) and Reynold averaged Navier Stokes (RANS) are used together with finite rate chemistry modeling. Combustion behavior is investigated for different piston geometry with focus on wall heat losses. This thesis also discuss on the ignition sequence, which can potentially involve all three fundamental combustion modes as ignition wave propagation, premixed flame, and non-premixed flame. It is essential to understand how the mode of combustion changes, depending on the mixture composition, which is governed by engine parameters and fuel properties, in order to improve the modeling approach. This thesis also includes validation of the methanol spray modeling based on the experimental work in optical engines. In addition, a systematic survey for methanol chemical kinetic models is carried out.

In the second part of the thesis, numerical simulations are performed for the diesel spray combustion in a constant volume chamber. The goal is to investigate different air entrainment mechanisms and their effect on the oxidation of soot emissions depending on the distance between the fuel nozzle and the impingement wall.

1.3 Thesis contribution

The main findings of this work can be summarized as follows:

- The start of injection study revealed that methanol, in comparison to other fuels, requires much less time for premixing in order to achieve stratification level, resulting in partially premixed combustion. Injection timings between the SOI -30 and SOI -10 at low load, result in all fuel lean mixtures, and thus in, similar combustion type as in HCCI engines. The main reason for that is the low A/F_s ratio of methanol.
- The injection pressure study showed that methanol injected at TDC conditions with a high injection pressure will extend the ignition delay time due to the strong cooling effect. During that time, a premixed charge at stoichiometric mixtures will be formed. The auto-ignition of such mixture composition will give rise to a high rate of NO_x formation, which will produce more total NO_x emissions comparing to the low injection pressure cases, which resulted in typical CDC cycle.
- The piston geometry study implies that the post-injection flow which govern the local distribution of the hot combustion products, plays a key role in the optimization of the heat losses. A lower A/V ratio, meaning a reduced piston bowl area, does not always result in a lower wall heat losses.

- Ignition sequence analysis revealed that the ignition kernel of methanol starts within the fuel leanest mixtures, which is most likely caused by the cooling effect. It means that, by the time methanol fuel vapor reaches the correct temperature, enough for the auto-ignition, the ignitable mixture will become fuel leanest.
- The diesel spray-wall interaction study revealed that air entrainment mechanisms as flame lift-off length, impingement enhanced mixing and entrainment wave mixing are affected depending on the distance between the injector and the wall. It was found that the oxidation process of soot correlates with the air entrainment rate taking place after the end of injection. Wall impingement jets, with 30 mm and 50 mm distance to the wall, resulted in a higher air entrainment rate after the EOI and as a result faster soot oxidation in comparison to the free jet configuration.

1.4 Outline

Chapter 2 briefly presents the research carried out on LTC engines and some aspects of the diesel spray combustion, including more details for the research questions in this thesis. Chapter 3 includes governing equations and models describing reactive flows. Chapter 4 includes methods related to initializing, performing and post-processing of simulations together with a brief description of experimental methods. Chapter 5 includes a summary of findings for the methanol PPC studies. Chapter 6 includes summary of findings for the diesel impingement spray studies. Finally, Chapter 7 presents overall conclusions and future work.

Chapter 2

Compression ignition engines

2.1 Combustion concept

Combustion in compression ignition engines occurs through auto-ignition event which is forced due to the rapid increment of the pressure and temperature caused by the engine piston movement. The injection of fuel is introduced at different times relative to the piston position in order to achieve best possible combustion characteristics. The injection time will govern the mixture composition at the time of auto-ignition event and thus the chemical reactions responsible for emissions. Two main pollutants such as soot and NO_x emissions, are formed at a specific conditions described by fuel and air ratio ϕ and temperature. Classical $\phi - T$ diagram is used, see Figure 2.1, to identify mixture composition formed in different compression ignition concepts in relation to the soot and NO_x formation conditions. In the case of the conventional diesel combustion (CDC), where fuel injection is late and continues during the combustion process, mixture composition is located across both soot and NO_x peninsulas. It results in a high amount of these emissions and the need of the after-treatment systems. In order to avoid formation of soot and NO_x , the combustion temperature must decrease. One way to decrease combustion temperature is the exhaust gas recirculation (EGR) concept. Another, more challenging way, is advancing the start of injection which gives more premixing time for the fuel and air to achieve leaner composition and thus lower combustion temperature. The LTC concepts, such as HCCI, PPC and RCCI rely on the early injection timings. On the other hand, as the combustion temperature decreases, it may affect the combustion efficiency which will give rise to unburned hydrocarbons (UHC) and CO emissions. Therefore, research on the LTC engine concepts focus on understanding engine parameters, which control the mixture composition and thus emission output. At the same time, combustion characteristics as the pressure rise rate, combustion stability and engine load range need to be considered. Furthermore, due to the emission trade-offs, compromises between the emission output and efficiency are often needed.

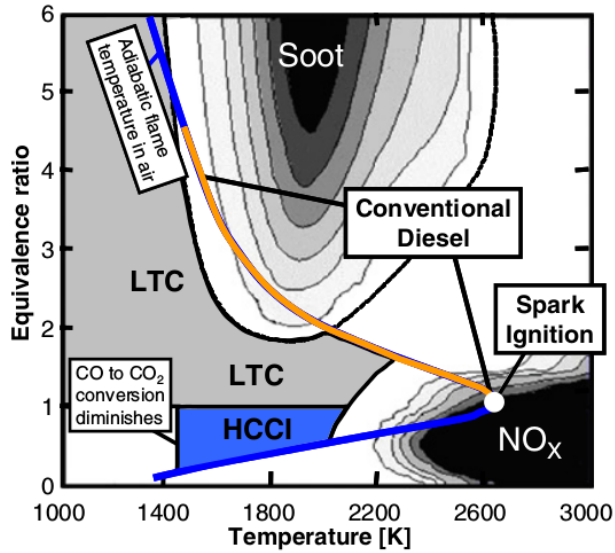


Figure 2.1: Operating regime in Φ - T space for different CI engine concepts. Adapted from [7, 9].

Detailed information from CFD simulations on mixture composition, combustion temperature and flame-wall interaction can be utilized to improve LTC engines. Figure 2.2 shows an example of a CFD simulation for compression ignition combustion with double injection strategy SOI-17/-3 aTDC. The highest temperature is in the location of stoichiometric mixtures (equivalence ratio equals unity in Figure 2.1). Stoichiometric mixtures are most often burned in diffusion flame mode, giving rise to emissions of NO_x . At the shown, CAD 5 aTDC, the diffusion flame of the main injection is attached to the piston wall, causing enhanced mixing, due to the large scale turbulent eddies. Turbulent flow results in a better air entrainment rate, that helps to reduce the emissions of soot, which are formed in the fuel-rich conditions located inside of the diffusion spray plumes. The low temperature zone, in-between the spray plumes, is originated from the pilot injection combustion (equivalence ratio below unity in Figure 2.1), taking place at an earlier CAD, which leads to reduced emissions of soot and NO_x , but may potentially cause more UHC and CO emissions. Multiple injection strategies are one of the advanced methods to alter mixture composition and mode of combustion in order to reduce total emission output.

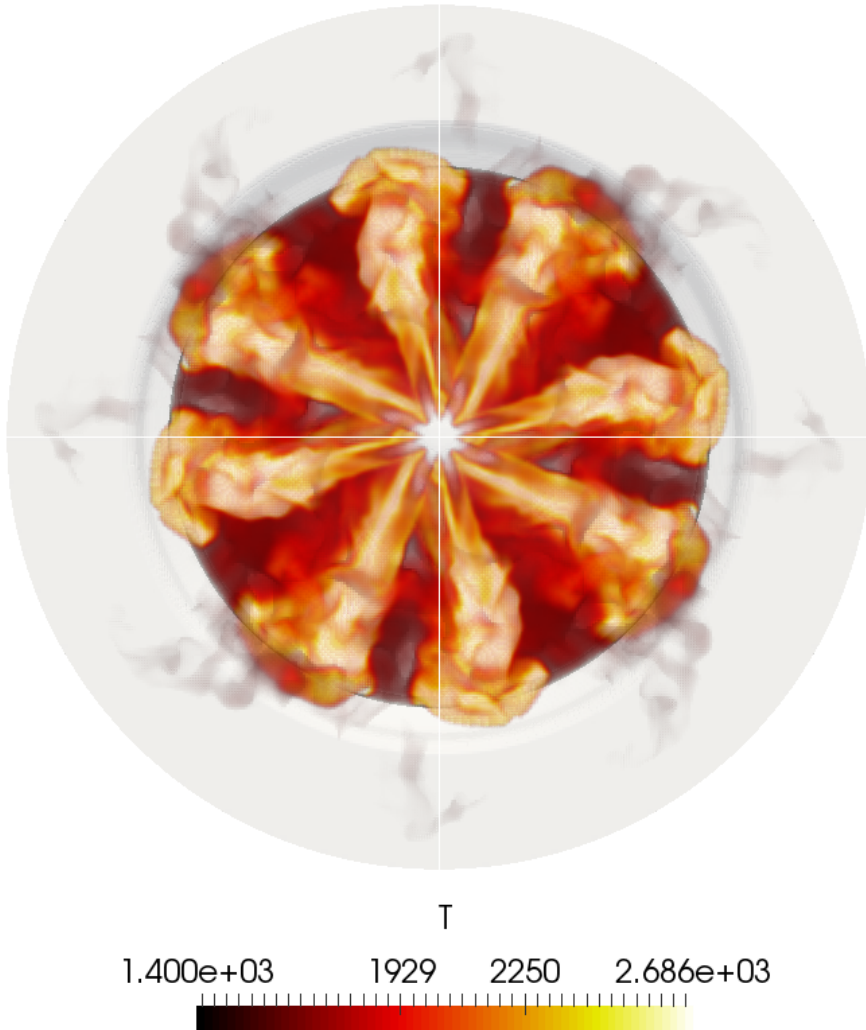


Figure 2.2: Volumetric temperature field at CAD 5 aTDC for double injection case SOI $-17/ -3$ of methanol combustion. Pilot injection resulted in low temperature combustion driven by ignition front propagation giving average temperature of 2000 K, typical for PPC engines. The main injection resulted in diffusion flame combustion typical for diesel engines giving stoichiometric temperature combustion of 2686 K. Too low combustion temperature give rise to unburned hydrocarbons (UHC) and carbon monoxide (CO) emissions. Too high temperatures gives rise to NO_x formation. The goal is to optimize combustion temperature by controlling mixture composition defined with equivalence ratio ϕ , and improve flame wall interaction to reduce heat losses. Depending on the fuel, soot can be formed in fuel rich pockets inside of the diffusion flames at temperatures between 1600K-2200K. Simulation and rendering performed by the author.

2.2 Partially premixed combustion engines

One of the promising LTC engine concepts is PPC. The main reason why the PPC concept is attractive, is the emissions window in the CO/HC-NO_x trade-off. Between approximately SOI -40 and SOI -25 aTDC combustion results in a low emission output of both HC/CO and NO_x [10]. The emission window depends on the mixture composition that gives rise to low enough combustion temperature to avoid NO_x formation, but at the same time, a high enough combustion temperature to complete conversion of HC and CO. The second advantage of PPC engines is reduced wall heat losses, which contributes to a high indicated gross efficiency. The performance studies by Manente et al. [11–13] and Kalghatgi et al. [14] for gasoline PPC engines for different setups and engine operation points show the advantages over CDC engines both in emission output and indicated gross efficiency.

The main challenge is the limited load range due to the pressure rise rate caused by the combustion in the premixed mode, especially at higher loads. In addition, extreme inlet conditions required at certain conditions to initiate auto-ignition event, are not feasible in real engine applications. Many studies were conducted in order to extend the operation range by utilizing fuels with different RON numbers [15, 16]. The stability of combustion is mostly sensitive to the inlet temperature. A number of solutions were proposed to improve it, as for example glow plugs [17] or fuel blends with a specific reactivity (RCCI engines)[18].

The definition of PPC regime is not always consistent in the literature. The main goal of the PPC concept is to find the optimal emission window by controlling mixture composition with various engine parameters. However, the stratification level of the fuel/air mixture needed to achieve that emission window is not strictly defined and may be significantly different depending on the fuel properties and the engine parameters.

In order to gain more in sight, combustion phenomena in PPC engines is extensively investigated in optical engines setups [19–23]. Laser diagnostics are employed to study spatial and temporal distribution of the fuel and combustion radicals. The challenge is to understand the structure of the reaction zone and to quantify mixture composition. In PPC engines, all three fundamental combustion modes can co-exist, which are ignition front propagation, premixed flame and non-premixed flame. From the numerical point of view, it is important to know which combustion mode is acting, due to the challenges associated with the combustion modeling. In this work focus is set on the transition between premixed and non-premixed combustion. Investigating the difference between the ignition front and premixed flame is more challenging and often requires detailed numerical simulation (DNS). More discussion is provided in section 2.3.

One PPC definition presented by Musculus et al. [8], shows that the injection timing in PPC should be advanced so that the majority of the fuel is consumed in the premixed

combustion mode, while only small remaining part of the fuel is consumed in the non-premixed mode. Figure 2.3 shows a conceptual model for the CDC and PPC ignition sequence.

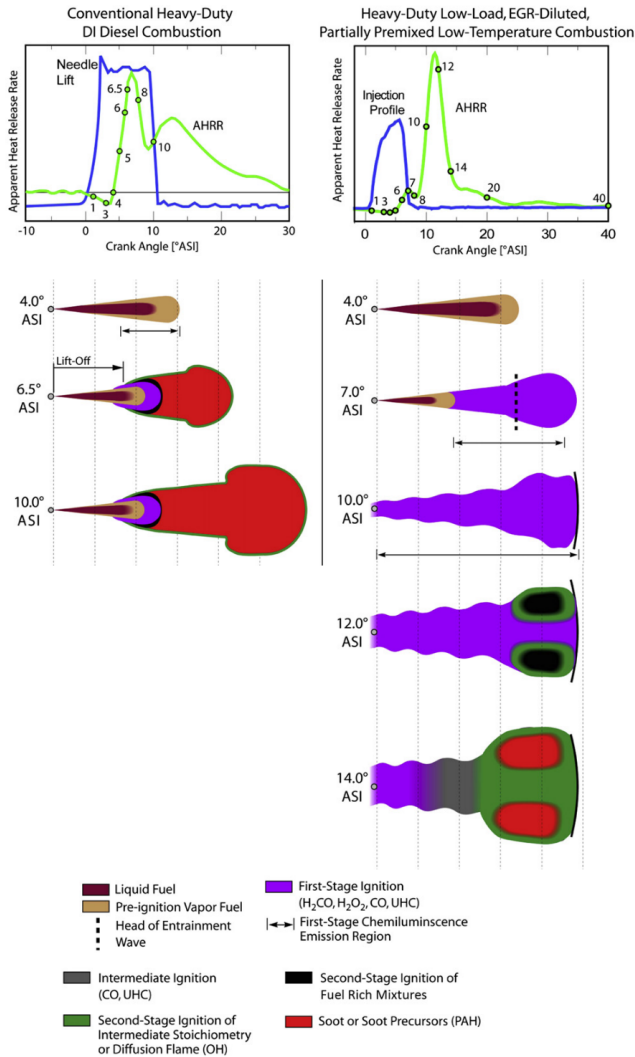


Figure 2.3: Phenomenological models for CDC and PPC. Reproduced from [8].

Another PPC definition is based on the mixing period time (MPT), which is the time between the end of injection (EOI) and the start of combustion (SOC).

$$MPT = SOC - EOI \quad (2.1)$$

If the mixing period time is positive, then a certain operation point is categorized as PPC. This rule would apply for the presented PPC pressure trace in Figure 2.3, where mixing

period time is positive. The drawback of the MPT definition is that it lacks the information on the stratification level. For example, if the mixing period time is long enough, the mixture composition may result in all fuel lean mixtures, leading to premixed combustion mode only, similar to that in HCCI engines. As the mixing period time gets shorter, mixture composition will start to include local fuel rich mixtures, which will lead to a mixed combustion mode consisting of both the premixed mode and non-premixed mode, as in Musculus conceptual PPC model. Furthermore, even if the mixing period time is no longer positive (meaning that injection is ongoing during the combustion), it is still possible to achieve the premixed dominant combustion, which is consistent with Musculus conceptual model, but inconsistent with the MPT rule.

The information about mixture composition is especially helpful for the early injection cases. Mixing controlled combustion is characterized by fluctuations in the heat release trace, but for the early injection times (positive MPT), it may be difficult to determine if fluctuations are related to the mixing controlled combustion. Thereby, it is difficult to determine if local fuel rich mixtures exist in the domain during combustion.

The mixture composition at a given start of injection can vary depending on the engine load or EGR content, but most importantly on the fuel mixing properties, which in case of methanol, are quite different from other conventional fuels. For example, start of injection studies for gasoline PPC engines in Refs. [24–26], shows that composition of fuel lean and fuel rich mixtures for gasoline is achieved at around SOI -60 aTDC. In the case of methanol, the combination of fuel lean and fuel rich mixtures is achieved at much later SOIs, e.g., SOI -5 assuming comparable ambient conditions. Mixing properties of methanol in PPC engines are addressed and discussed in this thesis.

2.2.1 Methanol as a PPC engine fuel

Methanol, as an alternative fuel, is being applied in a number of pilot projects for city buses and ferries. It became an interesting choice on the alternative fuel market due to several things. The unique thermodynamic properties cause a severe cooling effect and prolonged ignition delay time that can be both positive and negative for the performance in LTC engines. The main advantage is that methanol has almost non-sooting combustion and can be extracted in renewable production loops based on the biomass, which can contribute to a lower net CO₂ emissions [27]. On the other hand, ongoing research is also focusing on dealing with corrosive properties of methanol, as well as on a detailed emission analysis related to particulate matter [28].

Most recently methanol was investigated in compression ignition engines under PPC conditions. Studies show that methanol results in a low emission output, fulfilling the EURO

IV standards without using any after-treatment systems [29, 30]. Single cylinder engine experiments with a high compression ratio showed indicated gross efficiency up to 53% [31]. Numerical studies on full engine systems imply a higher gas exchange efficiency compared to gasoline, which improves overall brake thermal efficiency [32, 33]. Methanol oxygen demand to achieve stoichiometry is only half of that for gasoline. Thus, the mixing time to achieve optimal PPC mixture composition is short. The penalty is the high latent heat of vaporization which sets demand for a high intake temperature and relative low energy density. Selected properties of methanol, gasoline and diesel are given in Table 2.1.

Table 2.1: Selected fuel properties [34].

	Q_{LVH} [MJ/kg]	A/F_s	Latent heat of vaporization [kJ/kg]
methanol	20	6.47	1103
gasoline	44	14.6	350
diesel	43.2	14.5	270

An example of heat release trace for methanol PPC is presented in Figure 2.4. It is shown that despite negative MPT, the majority of the fuel is combusted in the premixed combustion mode. Other fuels such as gasoline or diesel, injected at the identical conditions, would result in a larger contribution of the mixing controlled combustion, typical for CDC, due to the shorter ignition delay time. Therefore, the SOI interval for achieving methanol PPC can be located much closer to the top-dead-center (TDC) compared to gasoline or diesel fuel.

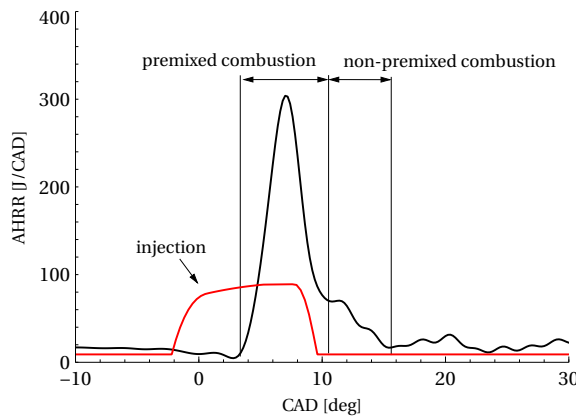


Figure 2.4: Schematic heat release diagram for methanol PPC engine concept with negative MPT. Specifications: SOI -2.2 aTDC, P_{inj} = 800 bar, P_{in} = 1.56 bar, T_{in} = 416K, $IMEP_g$ = 3.4 bar. Sara Lönn is acknowledged for providing engine data.

Another example of heat release rate is presented for a comparable engine operation point

between methanol and primary reference fuel (PRF100). The SOI, CA50, engine load IMEP_g and injection pressure are fixed. Instead, the intake temperature and the injection duration are used for calibration. Figure 2.5 shows heat release rate and mixing line at TDC. One can note that mixture composition in case of methanol became significantly leaner and colder compared to PRF100. Based on the heat release rate, one can approximate that methanol resulted in almost negligible amount of mixing controlled combustion, meaning all fuel lean conditions, whereas PRF100 still may contain both fuel lean and fuel rich mixtures, which give rise to the mixing controlled combustion. More discussion on the stratification level and the mode of combustion in methanol PPC engines are presented in Paper I and Paper V.

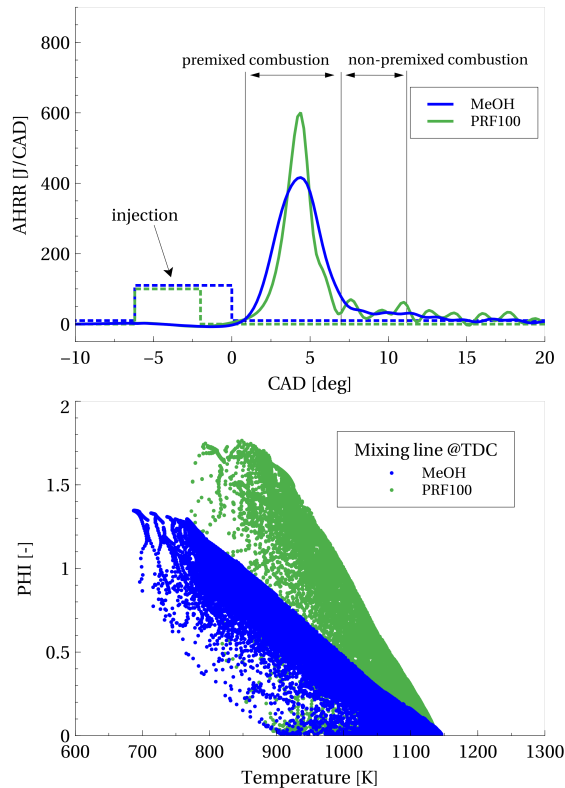


Figure 2.5: Mixing line for methanol (MeOH) and primary reference fuel (PRF100) under comparable engine operation point: $IMEP_g=3.55/3.58$, $CA50 = 2.76/2.72$, $P_{in} = 1.25/1.25$ bar , $m_f = 99mg/41mg$, $T_{in} = 174K/158K$. Mixing line is taken at TDC based on non-reactive simulations performed by the author. Amir Bin Aziz is acknowledged for providing engine data.

2.3 Ignition front wave, premixed flame, non-premixed flame

The partially premixed combustion is a combination of the premixed combustion mode and the non-premixed combustion mode. The premixed combustion mode occurs when the fuel and oxidizer co-exist before the start of combustion either in a perfectly homogeneous field or in a stratified field that include either all fuel lean mixtures or all fuel rich mixtures. The non-premixed combustion occurs when the fuel and oxidizer must undergo mixing during the combustion, meaning that the fuel and oxidizer are introduced separately into the reaction zone. In the literature, however, PPC is also used as the indication of stratified conditions, regardless of whether the mode of combustion is pure premixed, or if it includes both premixed and non-premixed modes [35, 36].

In order to improve modeling of PPC engines in general, one must further distinguish between two different types of the premixed combustion, which are the ignition front propagation and the premixed flame front propagation.

The ignition front propagation is a sequence of local auto-ignition events that does not require the transport of mass and heat into the reaction zone. Instead, the reaction rates depends on the ignition delay time τ_{ig} governed by the local thermodynamic state including temperature, pressure and equivalence ratio.

$$\tau_{ig} = f(p, T, \phi) \quad (2.2)$$

Zel'dovic [37] proposed that the velocity of such ignition front propagation is proportional to the gradient of ignition delay time.

The premixed flame front propagation mode takes place if the transport of the heat and mass, in form of diffusion, into the reaction zone is necessary in order to continue the combustion process. The propagation of the premixed flame front is strongly affected by the turbulence structures, which is described in the well-known Borghi-diagram [35]. In the case of the ignition front propagation, the effect of turbulence is indirect, meaning that the turbulence, governs the mixing process and thus the distribution of the local temperature and equivalence ratio ϕ prior to ignition. During combustion, the integral turbulent time scale is slower than chemistry time scale.

The most common numerical practice in order to distinguish between ignition and flame mode, is the budget term analysis, where chemistry source term is compared with the diffusion term in the species equation. The dominance of the chemistry source term would imply ignition front mode. A balance between the chemistry source term and the diffusion term would imply flame propagation mode. Budget terms studies for PPC related conditions were performed in the DNS framework, which showed that ignition front and

premixed flames can occur at the same time, but the ignition mode is most likely the dominant mode of combustion [38–41].

Since PPC engine may involve all three fundamental combustion modes, ignition, premixed flame, and non-premixed flame, accurate simulations require advanced combustion modeling. Recently, Jangi et al. [42] performed methanol PPC engine simulations using advanced modeling approach called Eulerian Stochastic Fields (ESF), where it was noted that for strongly stratified conditions well-stirred-reactor (WSR) approach fails to predict combustion process compared to the ESF model.

In the case of HCCI engines, where combustion takes place at much more homogeneous mixtures compared to PPC, the dominant mode of combustion is pure ignition wave mode. In this case, a combustion model is not necessary and most often the WSR approach is used, which calculates reaction rates based on the resolved part of the flow.

In the case of CDC engines, the dominant mode of combustion is the non-premixed flame. In this type of combustion, combustion models is important due to the insufficient spatial resolution to resolve the thin reaction zone layer between the oxidizer side and the fuel side. Many different approaches have been developed to account for the sub-grid modeling. Chomiak and Karlsson [43] proposed partially stirred reactor model (PaSR), that would limit the reaction rates depending on the ratio between the chemical and turbulence time scales. Other approaches, such as eddy dissipation model (EDM), was proposed by Magnussen and Hjertager [44]. The mean reaction rate in EDM is based on the integral time scale mixing and the consumption rate of controlling species as fuel and oxygen.

Non-premixed combustion is also simulated with flamelet approach, where the reaction rates are pre-calculated and stored in the look-up tables [45]. Computational time is significantly reduced compared to the detailed chemistry simulations. Ongoing research is focusing on development of flamelet approaches such as Flamelet Generated Manifolds (FGM) method, in order to improve the ability to better predict ignition kernel at various conditions, including ignition phenomenon in LTC engine simulations [46–49].

Depending on the engine concept and the combustion mode, different combustion models must be employed. The combustion mode triangle in Figure 2.6 shows the contribution of each fundamental combustion mode in different combustion engine concepts.

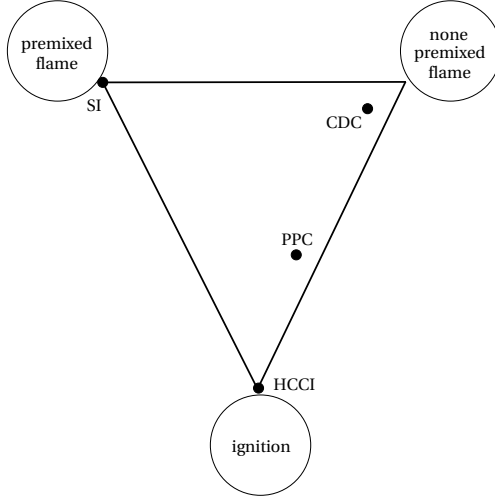


Figure 2.6: The combustion triangle divided into fundamental combustion modes. Engine concepts are located based on contribution of each combustion mode to the total heat release. Adopted from [50].

In Figure 2.6, PPC engine concept is located between the HCCI and CDC engine concepts. Depending on injection strategy, the level of the fuel stratification will vary, which also will cause different contribution to the total heat release from the premixed and the non-premixed combustion modes. It is expected that the importance of the combustion model will increase together with the level of the fuel stratification and the amount of the fuel rich mixtures. It is unclear at which stratification level the use of combustion model becomes necessary. The fuel stratification can be quantified by calculating distribution of local equivalence ratio defined as:

$$\phi = \left(\frac{m_f}{m_a}\right) / \left(\frac{m_f}{m_a}\right)_s, \quad (2.3)$$

where m_f is the local mass of the fuel, m_a is the local mass of the air, and s denotes stoichiometry. Values of $\phi > 1$ would then indicate fuel rich conditions, values of $\phi < 1$ would indicate fuel lean conditions, and value of $\phi = 1$ would indicate stoichiometric conditions. Figure 2.7 presents a conceptual allocation of the heat release with respect to the local equivalence ratio distribution and combustion mode based on the performed simulations in the thesis. It can be observed that stratification of ϕ in PPC concept is much broader, compared to HCCI engine concept, and thus, combustion models may play an important role.

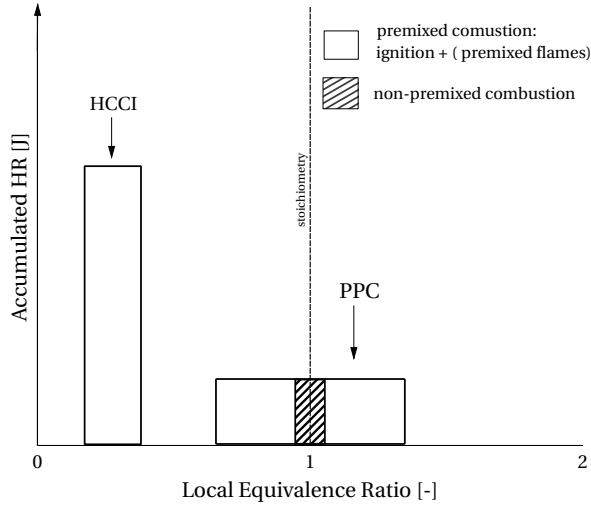


Figure 2.7: Proposed conceptual model of heat release distribution during combustion cycle depending on local equivalence ratio and mode of combustion.

2.4 Mixing mechanisms in Diesel sprays

During the last three decades, researchers continuously worked on improving understanding of the formation and oxidation processes of soot emissions in diesel sprays. Many important achievements have been accomplished within the engine combustion network (ECN) led by Sandia. The first conceptual model of a diesel spray structure was proposed by John Dec [51], where schematic distribution of soot, NO_x , diffusion flame and rich premixed flame zones was proposed. The flame lift-off length, which is the distance between the nozzle rim and nearest flame zone, was identified as the main region where the air entrainment mechanism is at work. The longer the flame lift-off length, the more air could enter the spray plume and reduce local equivalence ratio which would contribute to less soot [52]. Another mixing mechanism, entrainment wave, was identified by Musculus [53]. It was discovered that after the end of injection, oxygen is entering the spray plume from its tail at a much higher speed compared to the mixing rate taking place at the leading spray edge.

2.4.1 Impingement sprays

The goal is to maximize the air entrainment in a wall confined environment as the engine in-cylinder domain, hence research focus is also set on impingement diesel jets. Pickett and Lopez [54], presented optical measurements of soot mass in a constant volume vessel, for the free jet configuration and the wall jet configuration. They observed a significant reduction of soot emissions in the wall jet case and argued that soot mass reduction may depend on the mixing enhancement, i.e., oxidation or on the reduced soot formation due

to the wall cooling effect. Figure 2.8 shows diagram for the integrated soot mass and a schematic flow structure of impingement jet from their work.

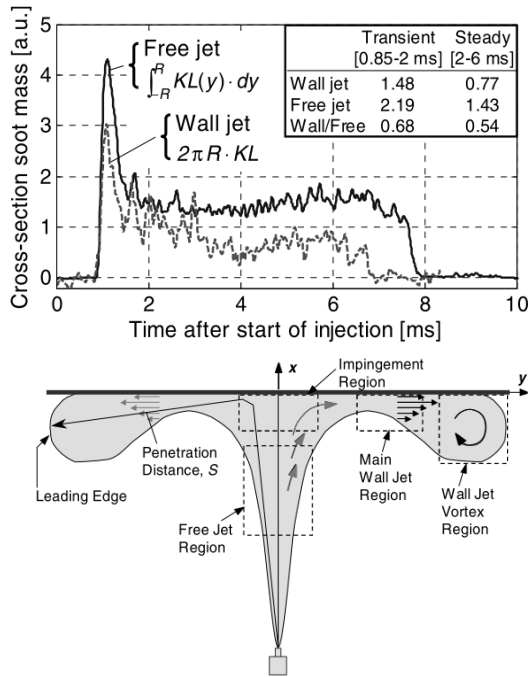


Figure 2.8: Integral of KL (soot mass) for two jet configurations and schematic wall-jet interaction flow structure. Reproduced from [54].

Other studies on impingement sprays were conducted by Bruneaux [55, 56]. Diesel sprays were investigated with the optical laser induced fluorescence (LIF) method to visualize distribution of low and high temperature combustion zones and distribution of poly-aromatic hydrocarbons (PAH) and soot. Based on the findings a conceptual model for the wall jet configuration, including the soot zone was proposed, Figure 2.9.

In Ref [57], Bruneaux focused on a detailed air entrainment analysis for diesel like gas injections with focus on the wall impingement. He concluded that air entrainment in the presence of the wall impingement can be locally increased. High intensity mixing would happen at the re-entrainment zone, as impingement vortex force fresh oxygen into the impingement zone. On the other hand, the overall entrained mass of air could be larger in the free jet configuration. Figure 2.10 shows the mixing intensity at three different regions for the wall jet case.

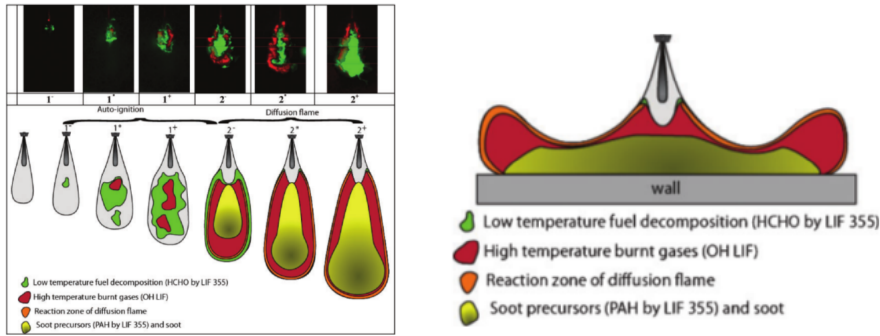


Figure 2.9: Conceptual model for diesel spray combustion in the free jet configuration (left) and the wall impingement configuration (right). Reproduced from [56].

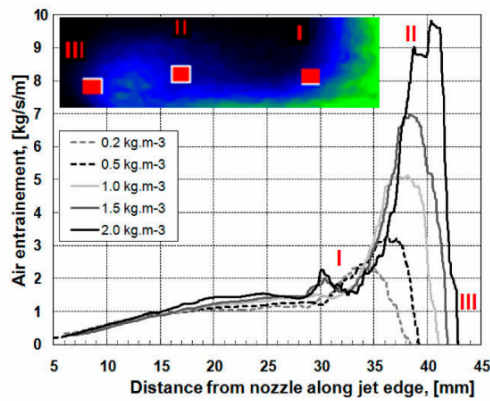


Figure 2.10: Bruneaux's air entrainment analysis for the impingement gas jet under diesel like conditions. Reproduced from [57].

Due to the multiple variables in the diesel wall impingement sprays such as the wall temperature, injection pressure, orifice size, injection duration, the wall curvature and the distance between the nozzle and the wall, the mechanisms governing wall mixing enhancement still require further investigation. Recently, CFD simulations were employed to study impingement diesel jets in RANS framework [58]. It was presented that wall modeling has a key effect on prediction of combustion characteristics. In this thesis LES approach is employed to investigate how different air entrainment mechanisms, such as flame lift-off length, wall impingement mixing and entrainment wave, are affected by changing the distance between the spray nozzle and planar wall, Paper VI.

2.4.2 Multiple injection strategies

Multiple injections are commonly used in engine applications. Early pilot injections are used to alter emissions of NO_x (similar to PPC engines) or to improve cold starts. Post

injections are used to support and complete the oxidation of fuel as the in-cylinder temperature drops due to the expansion stroke. The effect of double injections on the mixing rate was recently investigated by Hadadpour et al. [59, 60]. The performed numerical simulations of double injection strategies at various dwell times and injection durations imply that a shorter dwell time may decrease the air entrainment into the pilot spray plume, whereas it can be improved for the main injection, due to the perturbed and already reacting region, where the main injection is injected into. Multiple injections were also extensively studied in context of the wall impingement sprays by Maes et al. [61]. It was presented that shorter dwell times could reduce the final soot emissions formed in the main injection, which is in agreement with numerical findings of Hadadpour et al. mentioned above.

2.5 Development of combustion chamber

Piston geometry design plays a key role in the compression ignition engines such as PPC and CDC. The local turbulent flow caused by the spray-wall interaction, governs the air entrainment rate and distribution of chemical reactions and products. The piston bowl in CDC engines needs to be designed to maximize the enhancing of the mixing rate in order to deal with formation of soot. An example of that is the recently developed VOLVO's WAVE piston design. The soot oxidation process is improved, due to the jet-jet impingement vortex region, also called radial mixing zone (RMZ), which is amplified due to the additional piston curvature, which also resulted in a smaller impingement stagnation area [62–65]. LES studies in Paper VI, discuss on impingement vortex region and role in the air entrainment mechanisms for impingement sprays onto a planar wall. In the case of PPC engines, especially for methanol, soot emissions are much lower and thus optimization of the piston bowl shape can focus on wall heat transfer losses and combustion efficiency. Methanol, due to its properties, should achieve partially premixed conditions much faster than diesel or gasoline (low A/F_s). Thus, the injection timings can be postponed which would lead to better spray targeting, meaning all fuel injected into the piston bowl. In this thesis, a piston geometry study is performed for methanol PPC with late injection time. Focus is set on heat transfer analysis and overall wall heat losses, Paper III.

Chapter 3

Governing equations of reactive flows

Reactive fluids can be modeled by a set of transport equations. The formulation varies depending on the flow problem. In internal combustion engines, the flow is turbulent, reactive, and multi-phase including vapor and liquid phases. Governing equations for conservation of mass, momentum, energy and species for the vapor phase can be written as:

$$\frac{\partial \rho}{\partial t} + \frac{\partial \rho u_j}{\partial x_j} = S_\rho, \quad (3.1)$$

$$\frac{\partial \rho u_i}{\partial t} + \frac{\partial \rho u_i u_j}{\partial x_j} = -\frac{\partial p}{\partial x_i} + \frac{\partial \tau_{ij}}{\partial x_j} + S_{u_i}, \quad (3.2)$$

$$\frac{\partial \rho h}{\partial t} + \frac{\partial \rho u_j h}{\partial x_j} = \frac{Dp}{Dt} - \frac{\partial J_j^h}{\partial x_j} + S_h, \quad (3.3)$$

$$\frac{\partial \rho Y_k}{\partial t} + \frac{\partial \rho u_j Y_k}{\partial x_j} = -\frac{\partial J_j^k}{\partial x_j} + \rho \dot{\omega}_k + S_{Y_k}, \quad (3.4)$$

where u , p , h and ρ denotes velocity, pressure, enthalpy and density respectively. Index i and j are vector index ($i, j = 1, 2, 3$) and k denotes chemical species ($k = 1, 2, \dots, N_s$). Y_k and $\dot{\omega}_k$ are the species mass fraction and chemical reaction rate of species k . Molecular fluxes of mass and heat J_j^k and J_j^h following Fick's and Fourier's law respectively are:

$$J_j^k = -\rho D_k \frac{\partial Y_k}{\partial x_j} \quad (3.5)$$

$$J_j^h = -\rho \alpha \frac{\partial h}{\partial x_j} \quad (3.6)$$

where D_k is the species diffusivity and α is the thermal diffusivity. τ_{ij} is the shear stress tensor. The strain rate τ_{ij} with viscosity μ is formulated as:

$$\tau_{ij} = \mu \left(\frac{\partial u_i}{\partial x_j} + \frac{\partial u_j}{\partial x_i} \right) - \frac{2}{3} \delta_{ij} \mu \frac{\partial u_k}{\partial x_k} \quad (3.7)$$

Enthalpy h states:

$$h = \sum_{k=1}^{N_s} Y_k h_k \quad (3.8)$$

$$h_k = h_{f,k}^0 + \int_{T_0}^T C_{p,k} dT \quad (3.9)$$

where $h_{f,k}^0$ is the enthalpy of formation at a reference temperature T_0 and specific heat capacity $C_{p,k}$. Equation of state is required to closure the above equations giving

$$p = \rho R_u T \sum_{k=1}^{N_s} \frac{Y_k}{W_k} \quad (3.10)$$

where R_u is the universal gas constant and W_k is molecular weight of species k with N_s as the total number of species. The source terms $S_\rho, S_{u_i}, S_h, S_{Y_k}$ account for the exchange rates between the vapor and the liquid phase.

3.1 Turbulence

Turbulent flows are characterized by scales describing different sizes and turn over times of eddies. The scales with highest energy content are the integral scales with characteristics length l_0 , velocity $u(l_0)$ and time τ_0 . Reynolds number are turn over time is defined as:

$$Re_0 = \frac{u_0 l_0}{\nu} \quad , \quad \tau_0 = \frac{l_0}{u_0} \quad (3.11)$$

where ν is kinematic viscosity. The smallest turbulent scales, Kolomogrov scales, describe eddies with the lowest energy content at the point where turbulent kinetic energy is dissipated into heat. Kolomogrov length, velocity and time scales are defined as

$$l_\eta = \left(\frac{\nu^3}{\varepsilon} \right)^{1/4} \quad , \quad u_\eta = (\nu \varepsilon)^{1/4} \quad , \quad \tau_\eta = \left(\frac{\nu}{\varepsilon} \right)^{(1/2)} \quad (3.12)$$

where ε is dissipation of turbulent kinetic energy. The energy cascade theory proposed by L.F Richardson explains the break down of the large eddies containing highest energy, into the smallest scales, Kolomogrov scales, by decreasing energy until they reach point of molecular diffusion and eventually dissipate into heat. The turbulence scales are modeled

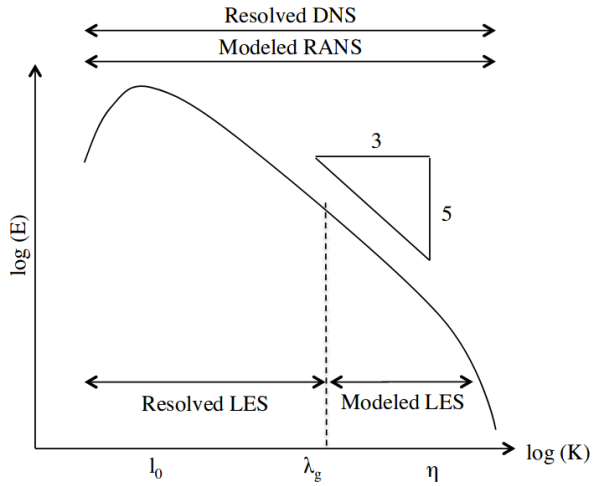


Figure 3.1: Schematic diagram of the resolved and modeled part of the turbulence kinetic energy spectrum for RANS, LES and DNS.

with two different approaches RANS and LES. Figure 3.1 shows energy cascade in relation to RANS and LES modeling.

3.1.1 U-RANS formulation

In U-RANS approach, a flow quantity ϕ can be decomposed into time averaged part $\bar{\phi}$ and fluctuating part ϕ'' as:

$$\phi = \bar{\phi} + \phi'' . \quad (3.13)$$

Due to the varying density in reacting flows Favre-formulation is employed

$$\tilde{\phi} = \frac{\bar{\rho}\phi}{\bar{\rho}} . \quad (3.14)$$

The time averaged U-RANS equations assuming $Le = 1$ are

$$\frac{\partial \bar{\rho}}{\partial t} + \frac{\partial \bar{\rho} \tilde{u}_j}{\partial x_j} = \bar{S}_\rho \quad (3.15)$$

$$\frac{\partial \bar{\rho} \tilde{u}_i}{\partial t} + \frac{\partial \bar{\rho} \tilde{u}_i \tilde{u}_j}{\partial x_j} = - \frac{\partial \bar{p}}{\partial x_i} + \frac{\partial \bar{\tau}_{ij}}{\partial x_j} - \frac{\partial \widetilde{\bar{\rho} u_i'' u_j''}}{\partial x_j} + \bar{S}_{u_i} \quad (3.16)$$

$$\frac{\partial \bar{\rho} \tilde{h}}{\partial t} + \frac{\partial \bar{\rho} \tilde{u}_j \tilde{h}}{\partial x_j} = - \frac{\partial \bar{p}}{\partial t} + \frac{\partial}{\partial x_j} \left(\bar{\rho} \tilde{\alpha} \frac{\partial \tilde{h}}{\partial x_j} \right) - \frac{\partial \widetilde{\bar{\rho} h'' u_j''}}{\partial x_j} + \bar{S}_h \quad (3.17)$$

$$\frac{\partial \bar{\rho} \tilde{Y}_k}{\partial t} + \frac{\partial \bar{\rho} \tilde{u}_j \tilde{Y}_k}{\partial x_j} = \frac{\partial}{\partial x_j} \left(\bar{\rho} \tilde{D} \frac{\partial \tilde{Y}_k}{\partial x_j} \right) - \frac{\partial \widetilde{\bar{\rho} Y_k'' u_j''}}{\partial x_j} + \bar{\rho} \tilde{\omega}_k + \bar{S}_{Y_k} \quad (3.18)$$

According to Boussinesq assumption [66], Reynold's stress tensor can be written as:

$$-\widetilde{\bar{\rho} u_i'' u_j''} = \mu_t \left(\frac{\partial \tilde{u}_i}{\partial x_j} + \frac{\partial \tilde{u}_j}{\partial x_i} - \frac{2}{3} \frac{\partial \tilde{u}_k}{\partial x_k} \delta_{ij} \right) - \frac{2}{3} \bar{\rho} k \delta_{ij} \quad (3.19)$$

Turbulence models, such as well established $k - \epsilon$ model [67], are employed to provide information to calculate turbulent viscosity μ_t defined as:

$$\mu_t = \bar{\rho} C_\mu \frac{k^2}{\epsilon} \quad (3.20)$$

where k is turbulent kinetic energy, ϵ is dissipation rate and C_μ is model constant. The turbulent transport fluxes for mass and heat are modeled with gradient diffusion approach as:

$$-\widetilde{\bar{\rho} Y_k'' u_j''} = \frac{\nu^{sgs}}{Sc^{sgs}} \frac{\partial \tilde{Y}_k}{\partial x_j} , \quad (3.21)$$

$$-\widetilde{\bar{\rho} h'' u_j''} = \frac{\nu^{sgs}}{Pr^{sgs}} \frac{\partial \tilde{h}}{\partial x_j} . \quad (3.22)$$

The sub-grid Schmidt and Prandlt numbers are set to 0.7.

3.1.2 LES formulation

In LES approach a spatial filter G is used in order to resolve a certain range of turbulent scales. Filtered variable can be written as

$$\bar{\phi}(x, t) = \int G(r, x) \phi(x - r, t) dr, \quad (3.23)$$

where filter function G must satisfy normalization condition $\int G(r, x) dr = 1$. Favre-formulation is employed as

$$\tilde{\phi} = \frac{\overline{\rho\phi}}{\bar{\rho}}. \quad (3.24)$$

In LES, $\tilde{\phi}$ is the resolved part of the variable ϕ and ϕ'' is the unresolved part, i.e., sub-grid part. Governing equations for reactive multi-phase flow in LES framework can be formulated as:

$$\frac{\partial \bar{\rho}}{\partial t} + \frac{\partial \bar{\rho} \tilde{u}_j}{\partial x_j} = \bar{S}_\rho, \quad (3.25)$$

$$\frac{\partial \bar{\rho} \tilde{u}_i}{\partial t} + \frac{\partial}{\partial x_j} \left[\bar{\rho} \tilde{u}_i \tilde{u}_j - \bar{\tau}_{ij} - \tau_{ij}^{sgs} \right] = \bar{S}_{u_i}, \quad (3.26)$$

$$\frac{\partial \bar{\rho} \tilde{Y}_k}{\partial t} + \frac{\partial \bar{\rho} \tilde{u}_j \tilde{Y}_k}{\partial x_j} - \frac{\partial}{\partial x_j} \left[\bar{\rho} \tilde{D} \frac{\partial \tilde{Y}_k}{\partial x_j} + \Phi_{Y_k}^{sgs} \right] = \bar{S}_{Y_k} + \tilde{\omega}_k, \quad (3.27)$$

$$\frac{\partial \bar{\rho} \tilde{h}}{\partial t} + \frac{\partial \bar{\rho} \tilde{u}_j \tilde{h}}{\partial x_j} - \frac{\partial}{\partial x_j} \left[\bar{\rho} \tilde{\alpha} \frac{\partial \tilde{h}}{\partial x_j} + \Phi_h^{sgs} \right] = \frac{\partial p}{\partial t} + \bar{S}_h, \quad (3.28)$$

where \bar{S}_ρ , \bar{S}_{u_i} , \bar{S}_{Y_k} , \bar{S}_h are the filtered source terms for the mass, momentum, species and enthalpy equations between the gas and liquid phase.

The sub-grid terms, sgs-terms, still requires closure modeling. The filtered stress tensor is obtained from the resolved strained rate \tilde{S}_{ij} and pressure, using

$$\bar{\tau}_{ij} = -\bar{p} \delta_{ij} + 2\bar{\mu} \left(\tilde{S}_{ij} - 1/3 \tilde{S}_{kk} \delta_{ij} \right). \quad (3.29)$$

The sub-grid stress tensor τ^{sgs} is modeled using one-equation eddy model,

$$\tau_{ij}^{sgs} = 2\bar{\rho} \nu^{sgs} \left(\tilde{S}_{ij} - 1/3 \tilde{S}_{kk} \delta_{ij} \right) - 2/3 \bar{\rho} k^{sgs} \delta_{ij}, \quad (3.30)$$

where the sub-grid viscosity is modeled as

$$\nu^{sgs} = C_v \sqrt{k^{sgs}} \bar{\Delta}, \quad (3.31)$$

where $\bar{\Delta} = V_{cell}^{1/3}$.

The unresolved kinetic energy k^{sgs} is obtained from a transport equation

$$\frac{\partial \bar{\rho} k^{sgs}}{\partial t} + \frac{\partial \bar{\rho} \tilde{u}_j k^{sgs}}{\partial x_j} = \tau_{ij}^{sgs} \frac{\partial \tilde{u}_i}{\partial x_j} - D^{sgs} + \frac{\partial}{\partial x_j} \left(\bar{\rho} \frac{\nu^{sgs}}{Pr^{sgs}} \frac{\partial k^{sgs}}{\partial x_j} \right) + \dot{W}^s \quad (3.32)$$

where, \dot{W} is the spray induced turbulence term [68]. The dissipation of the sub-grid kinetic energy is modeled with

$$D^{sgs} = C_\epsilon \bar{\rho} k^{sgs 3/2} / \bar{\Delta}. \quad (3.33)$$

The model coefficients C_v and C_ϵ are set to 0.05 and 0.3 respectively based on Sone and Menon [69]. Closures for the sgs-terms are modeled using gradient-diffusion approach

$$\Phi_{Y_k}^{sgs} = \bar{\rho} \frac{\nu^{sgs}}{Sc^{sgs}} \frac{\partial \tilde{Y}_k}{\partial x_j}, \quad (3.34)$$

$$\Phi_{h_s}^{sgs} = \bar{\rho} \frac{\nu^{sgs}}{Pr^{sgs}} \frac{\partial \tilde{h}_s}{\partial x_j}. \quad (3.35)$$

Chemistry source term $\tilde{\omega}_k$ for species k in this thesis is treated with WSR and PaSR approach.

3.2 Turbulent combustion scales

Turbulent combustion is categorized with two none-dimensional numbers describing ratio between turbulent scales and chemical time scale τ_c . Damköhler number and Karlovitz number are defined as

$$Da = \frac{\tau_0}{\tau_c}, \quad Ka = \frac{\tau_c}{\tau_\eta} \quad (3.36)$$

Da and Ka numbers are mostly used to describe combustion behavior in premixed flames as in SI engines. A high Karlovitz number flow would imply that turbulent scales can disturb the inner layer of the flame reaction zone, leading to local quenching [70].

3.3 Mixture fraction and injection tracking

Mixture fraction Z is a key property in combustion research due to its conservation during combustion process [71]. It is defined as a ratio between the mass originated from the fuel m_f and the total mass in domain, where m_a is mass of the air, as:

$$Z = \frac{m_f}{m_f + m_a} \quad (3.37)$$

In this thesis mixture fraction Z is calculated from a transport equation, where the fuel mass is added during injection time through the source term. Transport of Z gives the possibility to track the origin from each injection by adding multiple transport equations for mixture fraction Z_{inj} , see Eqn. 3.38. The spray source term $\bar{S}_{Z_{inj}}$ in each Z_{inj} equation is activated during corresponding time of the liquid injection.

$$\frac{\partial \bar{\rho} \tilde{Z}_{inj}}{\partial t} + \frac{\partial \bar{\rho} \tilde{u}_j \tilde{Z}_{inj}}{\partial x_j} - \frac{\partial}{\partial x_j} \left[\bar{\rho} \tilde{D} \frac{\partial \tilde{Z}_{inj}}{\partial x_j} + \Phi_{Z_{inj}}^{sgs} \right] = \bar{S}_{Z_{inj}} \quad (3.38)$$

The total mixture fraction Z is then equal to the sum of all Z_{inj} . Furthermore, if no exhaust gas recirculation (EGR) is present, the mixture fraction can be used to calculate the local equivalence ratio as $\phi = [Z/(1-Z)]/[Z/(1-Z)]_{st}$. The sub-grid closure for the mixture fraction equation is modeled using the similar gradient diffusion approach

$$\Phi_{Z_{inj}}^{sgs} = \bar{\rho} \frac{\nu^{sgs}}{S_C^{sgs}} \frac{\partial \tilde{Z}_{inj}}{\partial x_j}. \quad (3.39)$$

3.4 Spray modeling

The liquid fuel injection models are of high importance in direct injection engines. A widely accepted formulation for liquid phase is called Lagrangian particle tracking (LPT). Liquid phase is represented by a number of parcels transported in the computational domain. Each parcel consists of a number of virtual droplets to mimic a massive number of droplets present in a real spray. Droplets in each parcel have a physical state specified with e.g. droplet size, temperature, composition and density. The position of parcels is coupled with the momentum equation in the gas phase. The exchange of heat and mass is coupled with the energy and species equations. Furthermore, the physical state of droplets is governed by various sub-models describing the break-up process and the evaporation process. The drawback of LPT method is the number of the involved sub-models and model constants [72]. The motion of a single parcel is governed by:

$$\frac{d}{dt} \bar{x}_p = \bar{u}_p \quad (3.40)$$

$$\frac{d}{dt} \bar{u}_p = \frac{C_D Re_p}{\tau_p 24} (\bar{u}_g - \bar{u}_p) \quad (3.41)$$

In the equations above, \bar{x}_p is the position vector of the parcel, \bar{u}_p is the velocity of the parcel, \bar{u}_g is the velocity of the gas, C_D is the drag coefficient. The parcel characteristic time scale is $\tau_p = d_p^2/18\nu$, where d_p is the diameter of parcel and ν is the gas-phase kinematic viscosity. The parcel Reynolds number is then $Re = |\bar{u}_{rel}|d_p/\nu$, with $\bar{u}_{rel} = (\bar{u}_g - \bar{u}_p)$. The drag coefficient is obtained from

$$C_D = \begin{cases} \frac{24}{Re_p} \left(1 + \frac{1}{6} Re_p^{2/3}\right), & Re_p \leq 1000 \\ 0.426 & , Re_p > 1000 \end{cases} \quad (3.42)$$

The brake-up process of droplets is based on WAVE theory [73], describing Kelvin-Helmholtz and Rayleigh-Taylor instabilities phenomena. The brake-up sub-models are then governing the size and the number of the droplet distribution due to the atomization. Heat and mass exchange between the liquid and gas phase are described with additional sub-models including e.g., Ranz-Marshall correlation [74].

In addition, much work has been reported in the literature for accurate modeling of the injection mass rate, which is of great importance especially for later injection timings. Measurements and modeling of injection mass rate was performed e.g, within Engine Combustion Network (ECN) [75], and recently by Xu et al. [76] and Aljohani et al. [77]. The LPT method is also sensitive to the grid size. The cell sizes between 0.25 mm - 0.125 mm are specified to be sufficient for typical spray engine applications [78, 79].

3.5 Combustion models

Chemical kinetics theory is used in order to model conversion of the chemical energy into the heat energy. A global reaction can be formulated as:



Such reaction is governed by reaction rate k calculated with Arrhenius formulation

$$k = AT^b \exp(-E_A/R_u T), \quad (3.44)$$

where A is a constant pre-exponential factor, E_A is the activation energy, R_u is the universal gas constant, and T is the temperature.

WSR

Following Arrhenius equation, the chemistry source term in the species equation can be formulated as:

$$\bar{\omega}_F = A \tilde{T}^b [\tilde{X}_F]^n [\tilde{X}_{Ox}]^m \exp(-E_A/R_u \tilde{T}) \quad (3.45)$$

The above formulation is based on the input from the resolved part of the flow i.e., no sub-grid combustion modeling is included. This type of approach, well-stirred-reactor (WSR)

approach, is commonly used if assumption of homogeneous conditions within a single CFD cell can be made. For a strongly stratified conditions, or for the premixed and the non-premixed flames, where reactions zones occur in thin layers, WSR approach is not preferable. Researchers are therefore focusing on combustion models that would consider chemistry-turbulence interaction, which is as important as it is challenging. In this thesis both WSR approach and partially-stirred-reactor (PaSR) are used for different PPC engine conditions.

PaSR

The partially stirred reactor approach proposed by Chomiak and Karlsson [43] is based on a fractal representation of the reaction zone in a CFD cell. It would mean that only a certain amount of charge inside of the cell is allowed to react. The reacting part is proportional to a ratio between chemical and mixing time scales τ_c and τ_{mix} as

$$\tilde{\omega}_k(T, Y_k) = \kappa \dot{\omega}_k(\tilde{Y}_k, \tilde{T}) \quad (3.46)$$

$$\kappa = \frac{\tau_c}{\tau_c + \tau_{mix}} \quad (3.47)$$

$$\tau_{mix} = C_{mix} \sqrt{\frac{k}{\epsilon} \left(\frac{\nu}{\epsilon}\right)^{1/2}} \quad (3.48)$$

Other combustion models based on PaSR approach were developed for instance by Sebelnikov and Fureby [80], where chemical time scale is related to the flame thickness, and applied for example in gas turbine burners [81]. Model proposed by Kong and Reitz [82] is a modified PaSR model where switch function is used based on the fuel stratification in order to dynamically judge if the reaction rate should be limited.

Eulerian transported PDF

The transported Eulerian PDF approach is advanced model with promising accuracy, although highly expensive. The mean reaction rate in each CFD cell is based on the multiple transport equations of each species that take into account the sub-grid turbulence. Depending on the number of stochastic fields, a PDF for reaction rates is calculated, rather than presumed. Number of studies were performed in order to investigate an optimal number of stochastic fields needed to obtain a sufficient PDF distribution in different combustion applications [42, 83–88].

3.6 Kinetics and speedup algorithms

The strength of the detailed chemistry simulations is the ability to better predict the timing and the position of ignition kernels, which is essential in modeling compression ignition combustion. However, depending on the size of the reaction mechanism, that describes the fuel kinetics, the computational cost will increase by the number of transport equations for included species, and by the number of reactions that chemical ODE solver needs to account for. Two common practices are used in order to reduce the computational cost. First one is the reduction of the chemical mechanisms by selecting only the most important reactions and species if possible. The other method is efficient calculation of reaction rates in the CFD domain using, for example, vector mapping technique called chemistry coordinate mapping (CCM). The chemistry calculation is accelerated by mapping a reactive composition of the CFD domain into a reduced-dimensional space based on the essential combustion variables such as T , Z , χ , Y_F temperature, mixture fraction, scalar dissipation rate and fuel mass fraction. Depending on the combustion application the number of required dimensions as well as discretization size may vary, which may give additional speedup [89, 90].

3.7 Numerical solver

The numerical simulations in this thesis were carried out using an open source CFD code, called OpenFOAM. The code is written in C++ language and is based on the finite-volume discretization. Due to the open-source licensing, OpenFOAM is known for its potential and flexibility for developing and implementing new solvers and models. Numerical schemes and algorithms are discussed in details for instance in Ref. [91].

Chapter 4

Methodology

This chapter will briefly touch on the work flow for performing simulations such as initial boundary conditions, grid construction, and post-processing tools as well as on the experimental methods used to generate validation data.

4.1 Grid techniques

The complication in the engine sector mesh generation is how different moving mesh techniques can be used to mimic the piston motion, and at the same time satisfy the grid requirements for the liquid spray. One of the available strategies is the "add and remove" technique developed by Polimi group [92]. In this method a layer of cells is added or removed, depending on the vertical stretching of the selected cells as the piston is moving. This way CFD cells within the liquid spray zone stays undeformed, which improves the accuracy and stability of simulation. The orientation of the CFD cells in relation to the spray injection angle is also improved. In Ref. [93] it has been presented that spray modeling give better results, if CFD cells are aligned with the spray direction. Alternative strategy is a uniform or tailored deformation of all cells i.e, "morphing". The drawback of morphing method is the potential requirement of re-mapping between the meshes as CFD cells become severely deformed, which decreases the accuracy of simulation. Third alternative, called immersed boundaries, uses topology of the piston to cut-off the Cartesian cells that are on the outside of the computational domain. This technique became popular due to better robustness and less effort for the grid preparation compared to the other two strategies. The drawback however, may appear due to the lower accuracy of the near wall modeling. Other technique related to the engine grid is the automatic mesh refinement (AMR) method [94]. As the name of the method suggests, the number of the cells in the domain would be optimized, by refining only the important part of the flow, depending on the specified conditions, e.g., temperature gradient or a certain reaction rate. This way it is not necessary to provide fine resolution in regions where the flow is not present at a

given time. In this thesis a combined strategy was used by employing a uniform morphing of the cells with the spray oriented alignment.

4.2 Boundary conditions

Performed engine simulations in this thesis deals with "closed-cycle" simulations, meaning the time between the intake valve close (IVC) and exhaust valve open (EVO). Thus, the challenge is to specify flow conditions caused by the intake valves. A common practice in closed-cycle simulations is to use solid-body rotation to represent swirl and tumble motions. Recently Ibrón et al. [95] investigated the effect of initial flow conditions for mixing process in PPC engines. It was presented that spray induced turbulence is much more dominant, than the turbulence originated from the intake valve flow. It implies that solid body rotation should be representative achieve intake-like flow. However, it was highlight that the sector assumption for PPC engines may fail due to the asymmetric mixing process, especially for advanced injection timings.

Other initial conditions are intake gas temperature and pressure, in-cylinder wall temperatures, mixture composition (in case of EGR) and swirl-number. In addition, boundary conditions for fuel injection needs to be specified, as fuel mass, injection rate, injection pressure, umbrella angle and start of injection.

4.3 Heat release rate analysis

Combustion cycle in engine experiments is analyzed with apparent heat release

$$\frac{\partial Q}{\partial \theta} = \frac{\gamma}{\gamma - 1} P \frac{\partial V}{\partial \theta} + \frac{1}{\gamma - 1} V \frac{\partial P}{\partial \theta} + \frac{\partial HT}{\partial \theta}, \quad (4.1)$$

where Q is the apparent heat release, γ is the specific heat capacity ratio, P is the in-cylinder pressure, V is the cylinder volume and HT is the wall heat losses [34]. The HT term is commonly modeled with Woschni approach [96], but other models are developed based on CFD and optical measurements of in-cylinder surface temperature [97–106].

4.4 Experimental methods

Experimental data performed by colleagues at Lund University was used to validate the simulated pressure trace and to calibrate spray models for the methanol PPC engine studies.

4.4.1 Metal engine experiments

Pressure traces are recorded by employing piezoelectric transducer located in the cylinder head. Based on the voltage amplitude, signal is converted to pressure every 0.2 CAD. AVL emission system was used to collect emissions.

4.4.2 Optical engine experiments

Validation of spray is performed based on the data obtained from Mie-scattering measurements and direct recording of natural luminosity. The optical engine is a modified heavy-duty Scania D13. The numerical reactive vapor phase is validated by comparing the natural luminosity signal by quantitative means. The origin of the natural luminosity signal is from molecules emitting spontaneous chemiluminescence as CH^* or OH^* [107]. The drawback of this method is a potential signal disturbance caused by the soot luminescence. A bandwidth filters are often used to filter unwanted source of the light. A more advanced method, planar laser induced fluorescence (PLIF), can be employed to specifically choose molecules of interest. In case of methanol combustion, soot emission are negligible, thereby natural luminosity signal is recorded by a high speed camera with no filters [108].

The liquid phase is compared with Mie-scattering measurements. A laser diode of 3 W at a wave length of 452 nm was employed. The laser light scattered from the fuel droplets was recorded by a high speed camera and post-processed to correct scattering caused by the piston bowl curvature [108].

4.4.3 Soot measurements

Laser diagnostics methods for Diesel combustion needs to deal with soot luminescence and interference of polycyclic aromatic hydrocarbons (PAH). The challenge is to distinguish between different sources of detected signal when comparing key radicals (OH , CH_2O) which can overlap with soot. Methods for detection and measurement of soot itself are in high focus within ECN, where CFD simulations are important tool to model and understand optically observed processes [94, 109–115].

Chapter 5

Results and discussion: methanol PPC engine

This chapter contains summary of numerical studies for the methanol PPC engine. Simulations are based on experiments performed in three different compression ratios; 15:1, 17.3:1 and 27:1. The effective compression ratio of optical engine is 16:1.

5.1 The role of start of injection

The start of injection is the main parameter controlling the mixing time of the fuel and air before the onset of ignition. Two numerical SOI sweeps were performed, in order to investigate the mixing process, ignition and the resulting combustion characteristics for methanol.

5.1.1 SOI sweep -20 to -3 at CR 15:1

A compression ratio of 15:1 was used in the first sweep, with SOI interval between SOI -20 aTDC to SOI -3 aTDC, Paper I. The investigated range of SOI is located close to TDC position, as it is expected that methanol will mix quickly for the lean mixtures due to the low $A/F_s = 6.47$. The pressure trace for the reference case SOI -17.5 is in good agreement with experiments after calibrating the inlet conditions. All investigated cases were calibrated afterwards using inlet temperature to achieve a comparable CA50. Here, the mixing process and ignition sequence is investigated for selected cases. Figure 5.1 shows the distribution of the temperature field and local equivalence ratio field for the SOI -17.5. Despite quite late injection timing, at onset of ignition, the mixture composition is located within $0.3 < \phi < 0.7$, meaning all fuel lean mixtures. Thus, the mode of combustion is the premixed mode, similar to that in the HCCI engines. Injected fuel interacts with the piston bowl creating an up-ward vortex, which pushes the fuel vapor towards the cylinder head. The ignition kernel starts at the leanest mixtures and propagates towards richer mixtures.

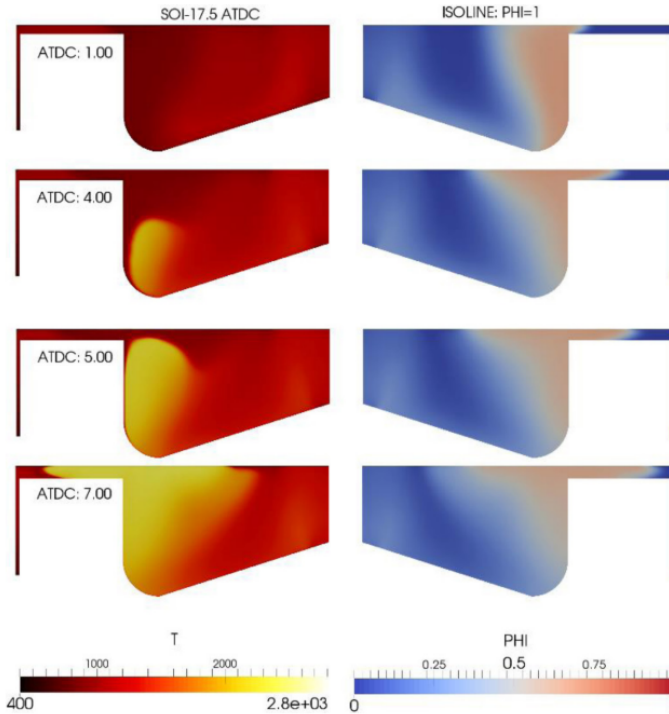


Figure 5.1: Temperature and equivalence ratio distribution for SOI -17.5 aTDC, $P_{in}=2.15$ bar, $T_{in}=452$ K.

As the injection time is delayed to SOI -3, the intake temperature required to match CA50 was increased by 28K. The resulted distribution of temperature and equivalence ratio is shown in Figure 5.2. The ignition sequence in this case is similar to that in a typical CDC cycle. A large part of the fuel will be premixed before the onset of ignition as a result of the mixing properties of methanol and the prolonged ignition delay time caused by the cooling effect. It means that the mixing controlled combustion, even at such late SOI, contributes much less to the total heat release. Moreover, the premixed mixtures had enough time to mix, close to, or below stoichiometry (solid white line). Thus, the resulted mixture composition in SOI -3, will give rise to a rapid pressure-rise-rate.

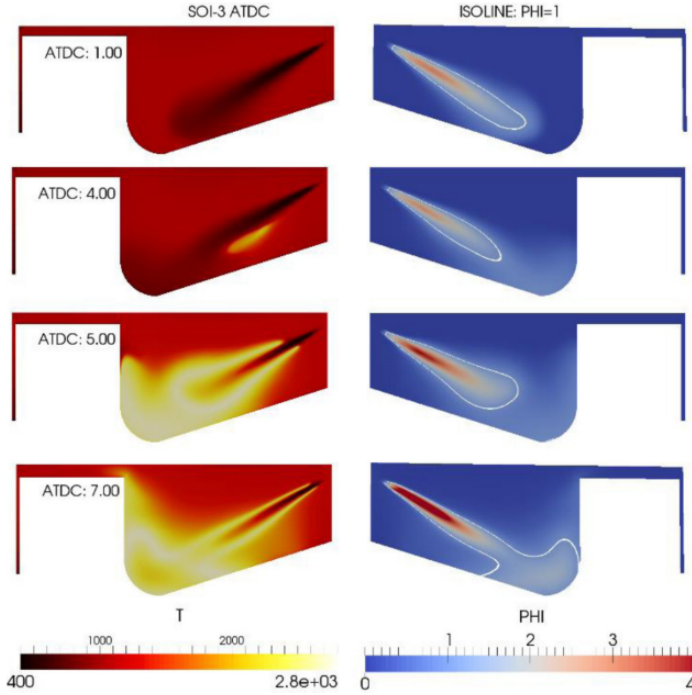


Figure 5.2: Temperature and equivalence ratio distribution for SOI -3.0 aDTC, $P_{in}=2.15$ bar, $T_{in}=480$ K.

As a consequence of delaying SOI, the premixed part of the fuel air mixture is reacting at increasingly richer mixtures. The local ignition delay time, $\tau_{ig} = f(p, T, \phi)$, for richer compositions will decrease (governed by chemical kinetic model) in comparison to leaner compositions, which will result in a shorter combustion duration, i.e., high pressure-rise-rate. The distribution of ignition delay times for various SOIs in PPC engines was recently investigated in Refs. [25, 116]. It was shown that stratification of ignition delay time for early injection cases (lean composition) is large due to the sensitivity to equivalence ratio ϕ . Large stratification of ignition delay time resulted in relatively longer combustion duration, i.e., slow propagation of ignition front. For the later injection timings (richer compositions), the stratification of ignition delay time is small. Due to a smaller stratification in ignition delay time, the richer composition, undergoes the auto-ignition sequence much faster, i.e., fast propagation of ignition front, leading to high pressure rise rate.

The maximal pressure rise rate for investigated methanol cases, as a function of SOI, is presented in Figure 5.3. Trend 1 shows increasing maximal pressure rise rate (MPRR) due to the premixed combustion that reacts at increasingly richer conditions towards stoichiometry. The reduction of MPRR, showed by Trend 2, depends on the decreasing ratio between the fuel mass burning in the premixed mode and fuel mass burning in the non-premixed mode.

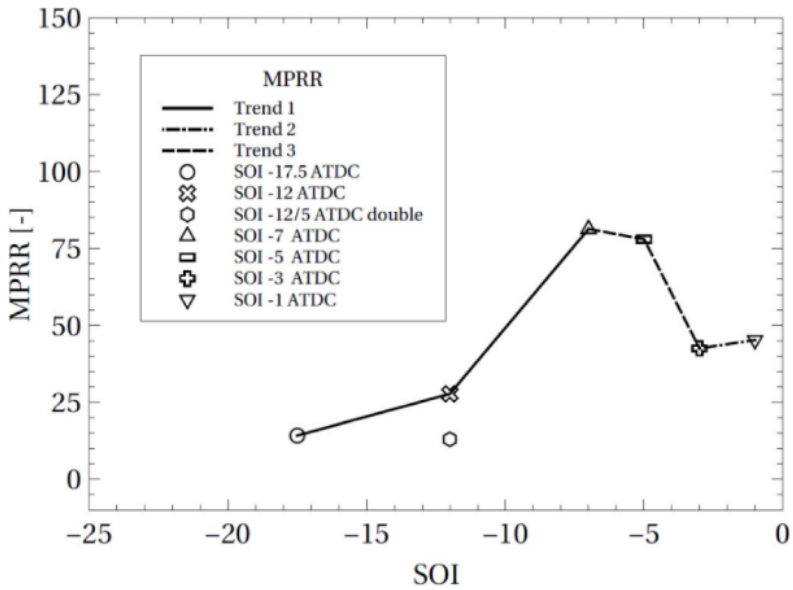


Figure 5.3: Maximal pressure rise rate as a function of SOI.

Other option to alter the mass ratio between the premixed and non-premixed combustion are double injection strategies. By setting the SOI time of pilot injection, one can control the richness of the pilot fuel and thus, the reaction front speed. The main injection is then combusted in the non-premixed combustion mode typical for CDC cycle. Figure 5.4 shows distribution of temperature and ϕ for the double injection case SOI -12/-5 aTDC that resulted in significant reduction of MPRR, cf. Figure 5.3.

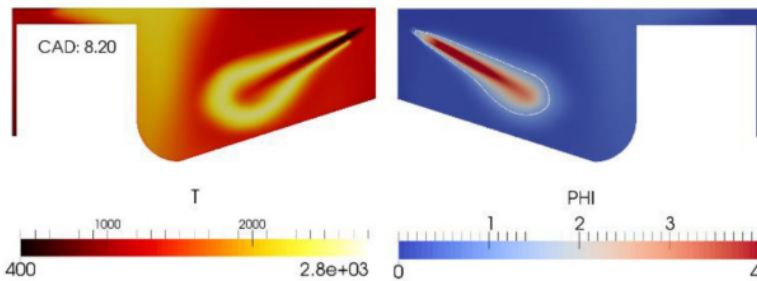


Figure 5.4: Distribution of temperature and local equivalence ratio at CA50 for double injection case SOI -12/5 aTDC, $P_{in}=2.15$, $T_{in}=456K$.

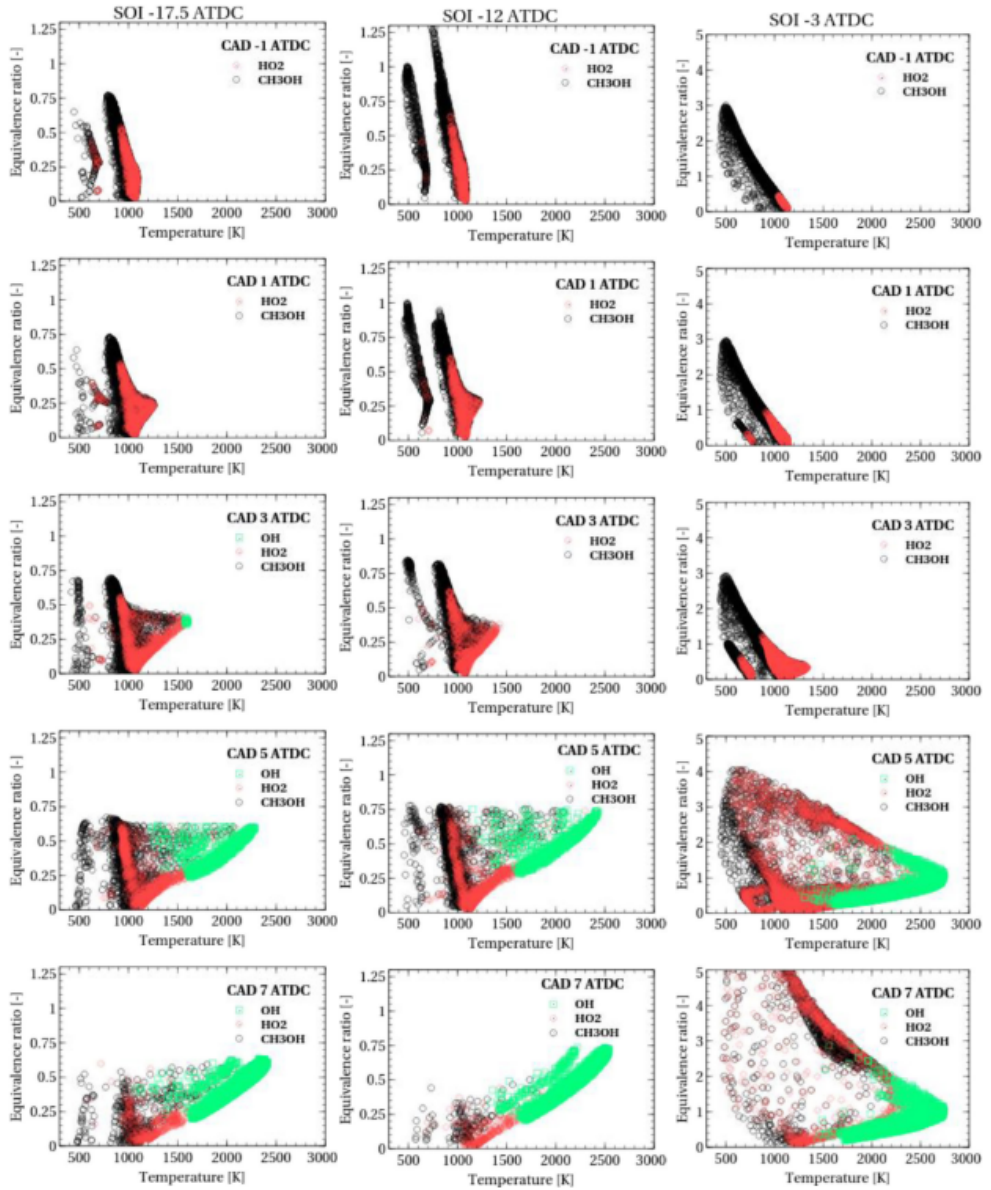


Figure 5.5: Ignition sequence analysis in ϕ - T space for SOI -17.5 aTDC, SOI -12 aTDC and SOI -3 aTDC.

The methanol ignition sequence in $\phi - T$ space is analyzed in Figure 5.5. All SOIs resulted in the ignition kernel taking place at similar fuel lean mixtures around $0.25 < \phi < 0.3$. Lean ignition kernels can be caused by the strong cooling effect of methanol, which limits the possibility of ignition at richer conditions. In case of gasoline PPC engine, the onset of ignition can occur at richer mixtures, due to the lack of the strong cooling effect [24]. The time necessary to increase the temperature of methanol, prolongs the mixing time prior to ignition. Figure 5.5, also shows that at CAD 5 aTDC, SOI -17.5 and SOI -12 resulted in all fuel lean mixtures, i.e., premixed combustion, while the diffusion flame manifold was achieved injection time as late as SOI -3.

5.1.2 SOI sweep -26 to -3 at CR 17.3:1

The second SOI sweep was performed in compression ratio 17.3:1 between SOI -26 aTDC and SOI -3 aTDC. The focus was set on the prediction of the pressure trace by using RANS-WSR approach and quantifying total heat release as a function of ϕ . The ignition delay time, needed to satisfy experimental CA50 condition, was achieved by calibration of the intake temperature. Figure 5.6 presents pressure trace comparison and allocation of the total heat release. It can be noted that the RANS-WSR approach performs well for the SOI -26 and SOI -16 as the distribution of heat release is located between lean mixtures achieving a small stratification level i.e., $0.25 < \phi < 0.5$. This level of stratification is typical for HCCI engines. RANS-WSR approach starts to over predict the pressure trace as the allocation of the heat release is more stratified as in SOI -11, i.e., $0.25 < \phi < 0.9$. The case of SOI -5 resulted in mixing controlled combustion, with majority of heat release at stoichiometry. It is worthwhile to highlight two things. One is that methanol combustion even at late injection timings burn in all fuel lean mixtures, giving rise to high MPRR, similar to previous section. Second is that over-prediction of pressure trace in SOI -11 can be due to the insufficient representation of mixing process by RANS, where fluctuations of local T and ϕ are averaged. The effect of the stratification level on the pressure trace prediction was also studied in Ref.[42]. It was presented that RANS-ESF approach could better predict ignition behavior.

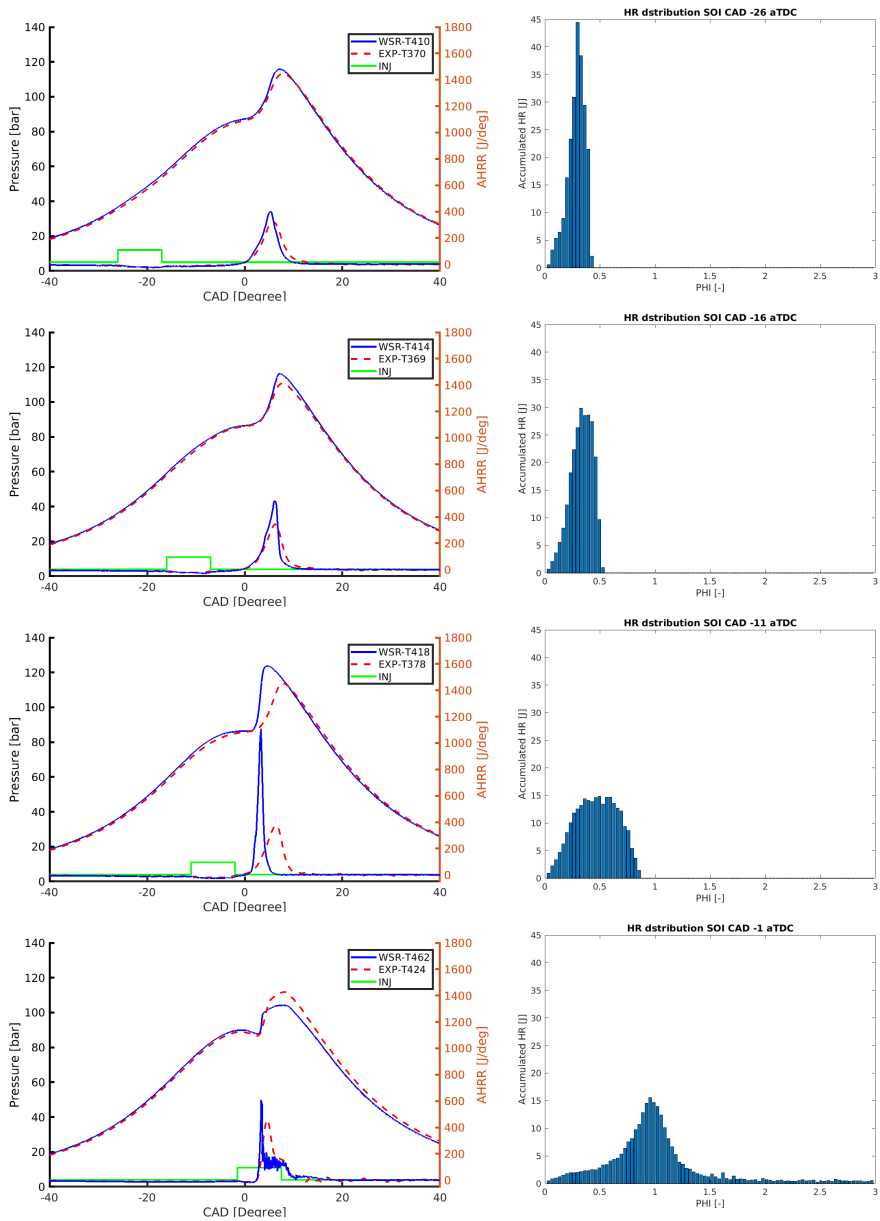


Figure 5.6: Pressure trace diagrams and allocation of total heat release as a function of ϕ for SOI sweep at compression ratio 17.3:1. Sam Shamun is acknowledged for providing experimental data.

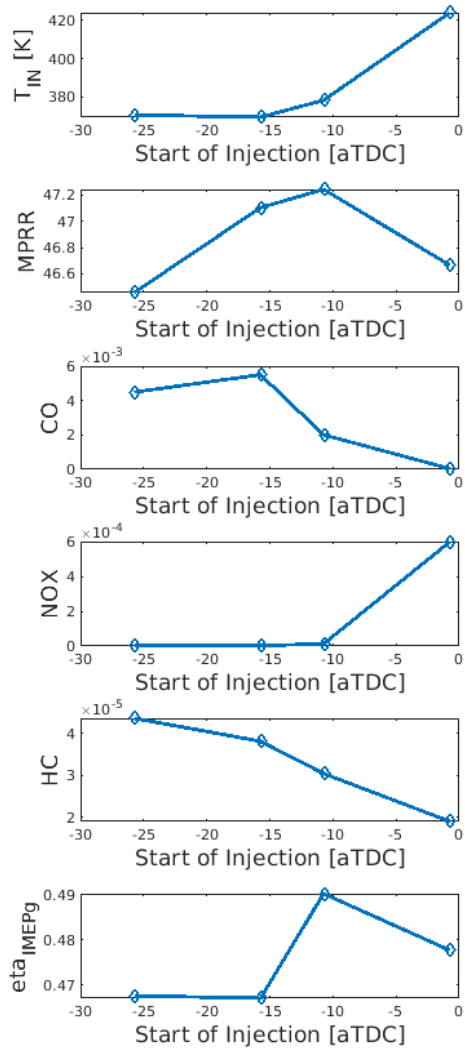


Figure 5.7: Engine performance from experiments for methanol engine with compression ratio 17.3:1. Sam Shamun is acknowledged for providing experimental data.

Combustion temperature is a function of ϕ , where stoichiometric mixtures $\phi = 1$ result in the highest combustion temperature. Thus, by analyzing distribution of allocated HR in plots in Figure 5.6, one can estimate the difference for the average combustion temperature between the cases. The combustion temperature, in next turn, govern the engine performance i.e., emission rates, combustion efficiency and the wall heat losses. Figure 5.7 shows the performance indicators for investigated SOIs. The trade-off between CO/HC and NO_x emissions, typical for PPC engines, is located at SOI -11. At the same time, the SOI -11 case, also resulted in the highest gross indicated efficiency. The reason is the total HR allocation, which is between $0.25 < \phi < 0.9$, that gives rise to a moderate combustion temperature. Cases SOI -16 and SOI -26 resulted in leaner combustion, and therefore worse conversion of HC and CO compared to the later SOI -11. The SOI -3 resulted in a CDC like cycle burning at high combustion temperature which caused more wall heat losses and NO_x emission. The penalty in case SOI -11, is the indication for the highest MPRR.

5.2 Effect of injection pressure on NO_x

The highest formation of NO_x during the combustion process, is located near the stoichiometric part of the charge, hence at the highest local combustion temperatures. In the experimental work of Shamun et al. [31], NO_x emission output was investigated for several engine parameters, e.g., injection pressure. It was observed that higher injection pressures could lead to a significant increment of NO_x emissions, when keeping constant CA50. Two numerical cases were chosen to investigate the underlying mechanism. A low injection pressure case of 800 bar that resulted in a typical Diesel cycle and a high injection pressure case of 1600 bar that resulted in typical PPC cycle, meaning premixed dominant combustion. As a result of the higher injection pressure, the injection duration was decreased to preserve the same amount of injected fuel.

Figure 5.8 shows pressure traces and distribution of the temperature and the equivalence ratio for these two cases during the ignition sequence. It can be observed that, at the onset of ignition, i.e., CAD 1.25 for the 800 bar case and CAD 6 for the 1600 bar case, the stoichiometric region of the spray plume, is much larger for the higher injection pressure case. The mixture composition containing a high amount of premixed charge at stoichiometric mixtures will result in a rapid combustion at high temperature and thus, an increased rate of NO_x formation. The reason for a longer ignition delay time in the high injection pressure case, is the cooling effect of methanol. The injection of high cetane number fuels, as diesel, would not result in a prolonged ignition delay time, due to the higher injection pressure.

The development of the hot gas mass fraction, indicating NO_x emissions and the modeled NO_x emissions, are plotted in Figure 5.9. The formation rate of NO_x in the high pressure injection case, "Case B", has a shorter duration, but at the same time, it has a higher slope,

which give rise to a higher total output of NO_x emissions. The hot gas mass fraction in the the domain corresponds well with modeled NO_x emissions.

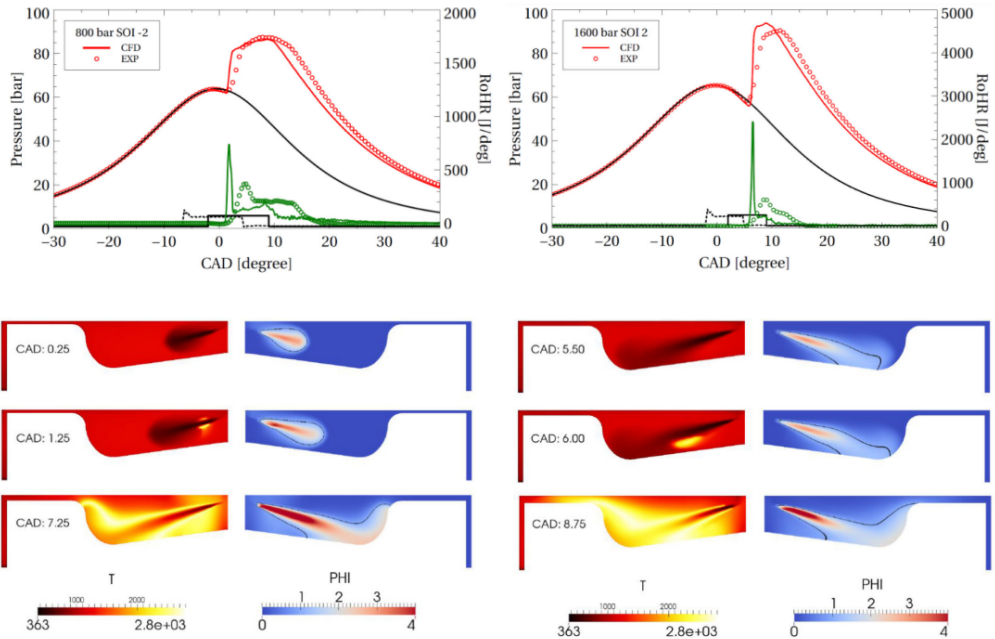


Figure 5.8: Pressure trace and distributions of fuel and temperature for 800 bar injection case (left column) and 1600 bar injection case (right column).

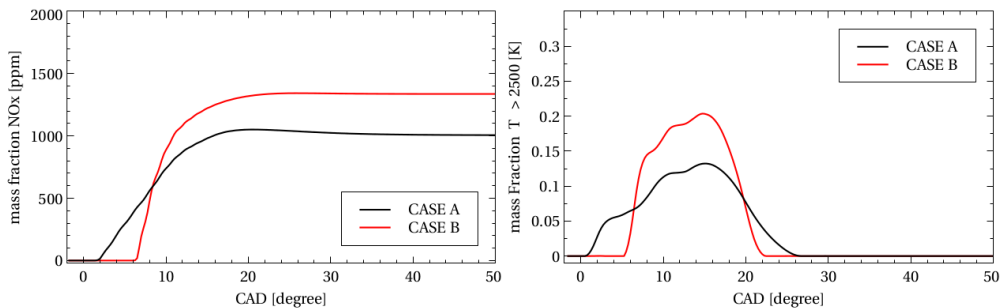


Figure 5.9: NO_x emissions (left); mass fraction of high temperature mass $T > 2500 \text{ K}$ (right).

The explanation for the higher total NO_x emission output, in the high injection pressure case, is the premixed dominant combustion at the stoichiometric mixtures. Furthermore, the results above imply that the PPC cycle, meaning premixed dominant combustion close to TDC, does not offer lower emissions of NO_x compared to diesel combustion cycle, i.e., dominant mixing controlled combustion.

5.3 Piston design study with focus on wall heat losses

The geometry of the piston bowl shape is one of the key features in developing cleaner combustion systems. In the case of PPC engines, efficiency may suffer from losses associated with the advanced injection timings that cause wall-wetting or fuel injections into the crevice volumes. Different combinations of piston concepts and injector types with narrower injector umbrella angles were proposed in order to improve combustion cycle. The piston design process involves optimization of emissions such as UHC, CO and soot [117–119], and optimization of the heat transfer [100, 120].

In case of methanol PPC, the injection time interval can be shifted towards TDC due to fast mixing with the air (low A/F_s ratio), helping to avoid losses associated with the crevice volumes. The mixing in diesel engines needs to be maximized by utilizing complex piston shapes to minimize sooting. In the case of methanol combustion, sooting is negligible and thus, the piston design approach can rather focus on the wall heat losses and combustion efficiency. A numerical piston design study was performed to focus on the heat transfer losses, Paper III.

It is of interest to investigate whether the area/volume ratio plays a role in the heat loss reduction, or if the spatial and temporal distribution of flow structures governing the temperature gradient, conductivity, contact area, and contact duration are more important. Simulation does not include thermal radiation. The piston geometry study is based on a single operation data point of SOI -1 CAD aTDC at low load, which resulted in premixed dominant combustion, fulfilling PPC conditions. Figure 5.10 shows the piston bowl designs and the distribution of the flow and temperature as a result of spray-wall interaction with different piston shapes. Piston G2 is used as the reference case as this piston design is used in the engine experiment. Modification of the piston is based on varying of the height and width, without changing the main curvature of the piston. Only piston G6, representing classical diesel piston with double leap design, has a different curvature.

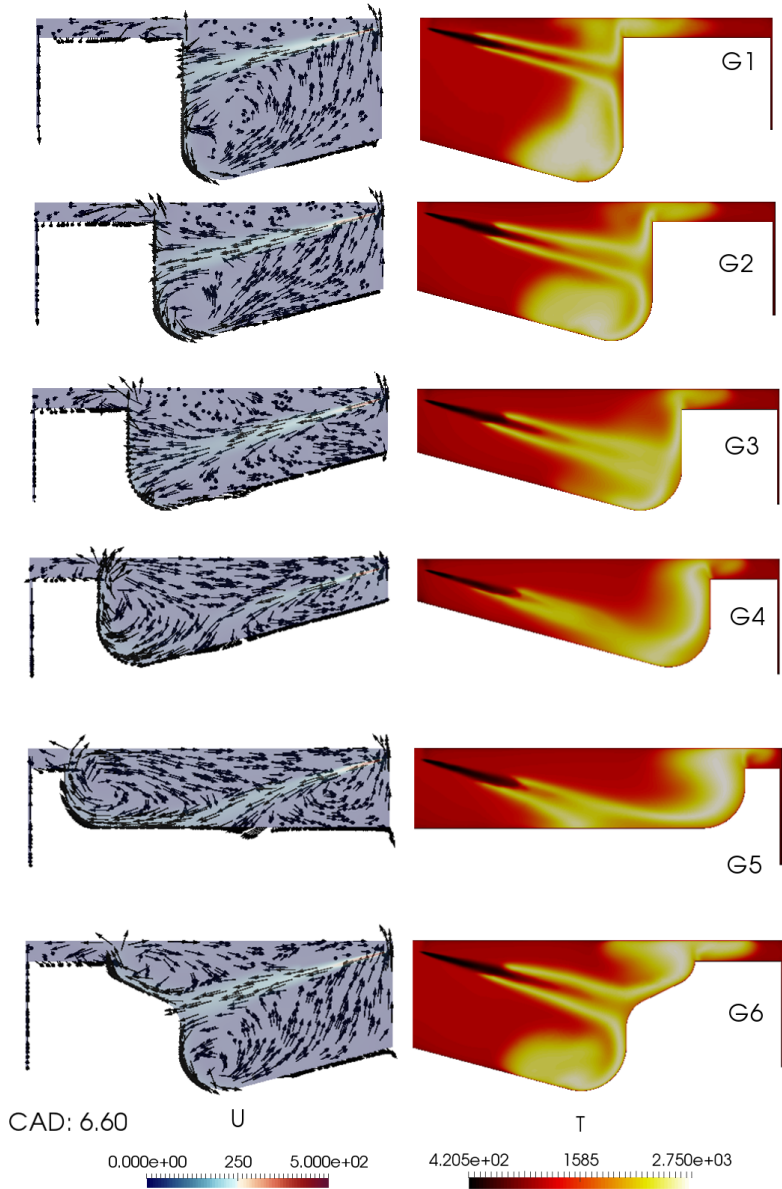


Figure 5.10: Flow structure and temperature distribution at CA50 for various piston designs. Piston G2 is the reference piston.

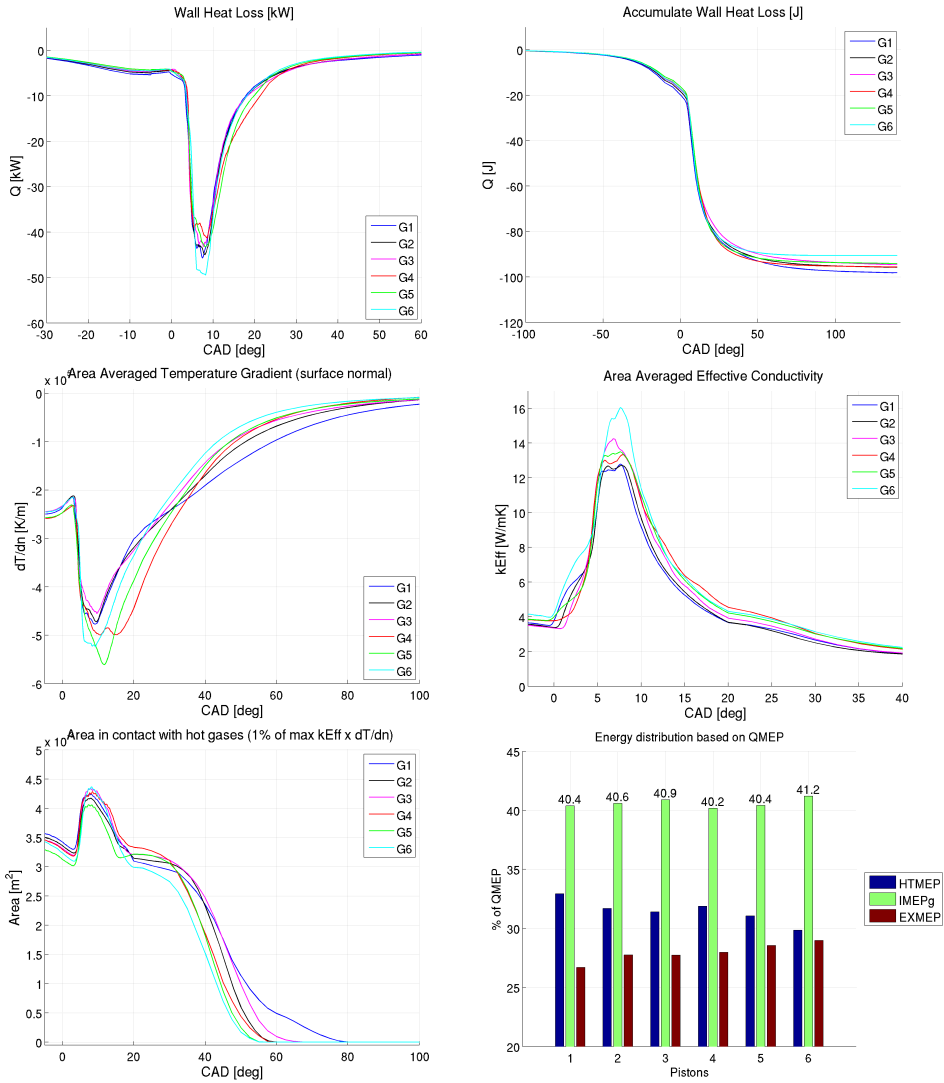


Figure 5.11: Wall heat loss analysis for different piston designs.

The analysis of the wall heat transfer, presented in Figure 5.11, shows the lowest accumulated wall heat loss for the piston G6. Piston G6, however, does not have the lowest area/volume ratio. In the analysis, surface averaged quantities for the temperature gradient, the effective conductivity and the size of the contact heat transfer area (hot gas wall region), were calculated and plotted against time. It can be observed that during the early combustion phase, between CAD 2 and CAD 30, accumulated wall heat losses are comparable. The difference arises during the late combustion cycle after CAD 30. It can be observed that both temperature gradient and the contact area are favorable in piston G6, which results in

the lowest total heat losses at the wall. The engine energy balance analysis, which also considers combustion efficiency that has an effect on the heat transfer, shows indicated gross efficiency of 41.2 % for piston G6 and 40.2 % for piston G4. Based on the results above, one can argue that the flow structures created due to the spray-wall interaction are more important than the area/volume ratio. The more effective way to reduce the wall heat losses is to create bulk flow that would push the hot combustion products, back to the inside of combustion chamber, i.e., away from the near-wall regions. Additionally, by moderating ignition delay time, or by designing a piston bowl, one could delay the onset of ignition, until the stoichiometric fuel vapor is distributed closer to the center of the piston volume, as a results of previous wall interaction.

5.4 Kinetic mechanisms

Comparison for different methanol kinetic mechanisms is carried out, Paper IV. The main conclusion is that the performance of the detailed kinetic models that include a large number of species and reactions, which are expected to deliver a high accuracy, varies compared to the experimental data for the ignition delay time and the laminar flame speed. The reduced versions or skeleton mechanisms originated from the detailed mechanisms show similar offset in ignition delay time and flame speed. The difference in the performance between the mechanisms, when used in the engine CFD simulations, leads to the tedious work for calibrating initial temperature conditions, in order to achieve correct combustion phasing. An non-realistic calibration of the intake temperature can also affect the accuracy of the predicted emissions rates.

Several detailed mechanisms and their corresponding reduced versions were tested, including Aramco Mech 2.0, Konnov mechanism, and Klippenstein mechanism (used as the main methanol mechanism in this thesis) [121–127]. Figure 5.12 shows the predicted ignition delay time at two different pressures of 20 atm and 50 atm at $\phi = 0.5$. The mechanism of Konnov over-predicts the ignition delay time at the presented conditions, compared to Aramco 2.0. However, the accuracy of each mechanism varies depending on the specified conditions. Thus, it is important to choose the mechanism that is "tailored" for conditions that matches a specific application.

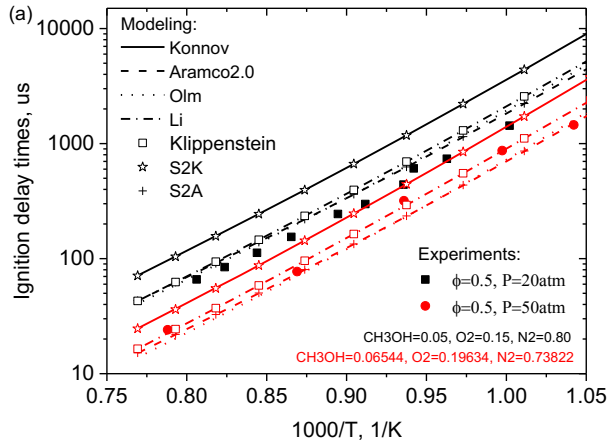


Figure 5.12: Ignition delay time for several detailed and reduced MeOH mechanisms computed in 0-D reactor.

The prediction for the laminar flame speed is presented in Figure 5.13. It can be noted that investigated mechanisms perform quite similarly for the fuel lean conditions. At the fuel rich conditions, the predicted laminar flame speed starts to deviate between different kinetic models. Similar to the ignition delay time, the Konnov mechanism gives faster flame speeds compared to other mechanisms.

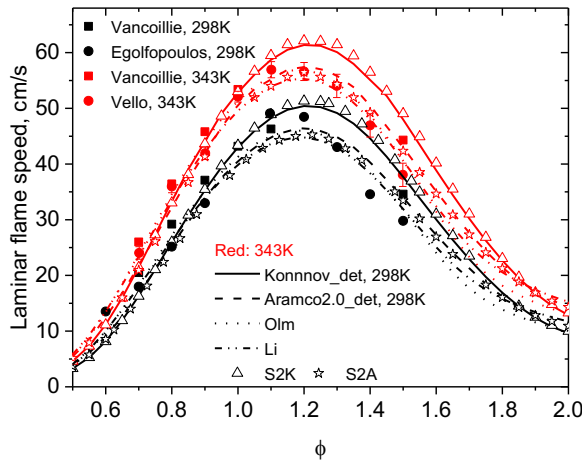


Figure 5.13: Laminar flame speed for several detailed and reduced MeOH mechanisms computed in 1-D solver.

Reduced mechanisms of Aramco and Konnov, with single-stage reduction (S1A, S1K) and double-stage reduction (S2A, S2K) and optimized mechanism of Klippenstein, were employed in engine simulations under HCCI conditions. The results shows a high sensitivity to the inlet conditions for correct prediction of pressure trace. Figure 5.14 shows the pressure traces at identical initial intake temperature of 457K for all tested mechanisms, which

resulted in a significant offset in the predicted pressure traces, i.e., 20 bar. Figure 5.15 shows the calibrated pressure traces by using the intake temperature. The maximal difference in the intake temperature requirement to match the pressure trace is 34K, which at TDC conditions (assuming adiabatic compression at CR 15:1) can lead to 100K difference.

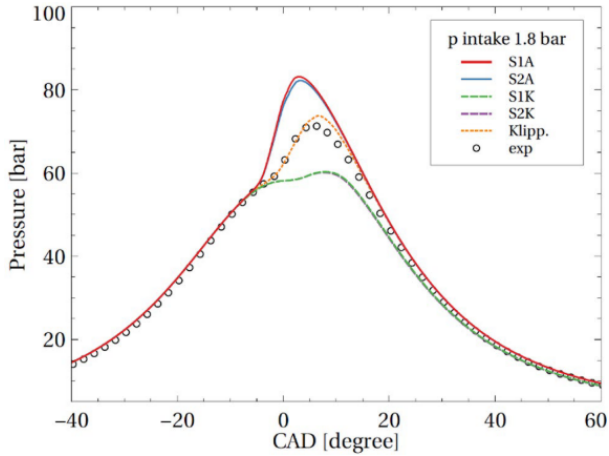


Figure 5.14: Pressure trace for several reduced MeOH kinetic models. Inlet conditions were calibrated for the Klippenstein mechanism, $T_{in} = 457\text{K}$.

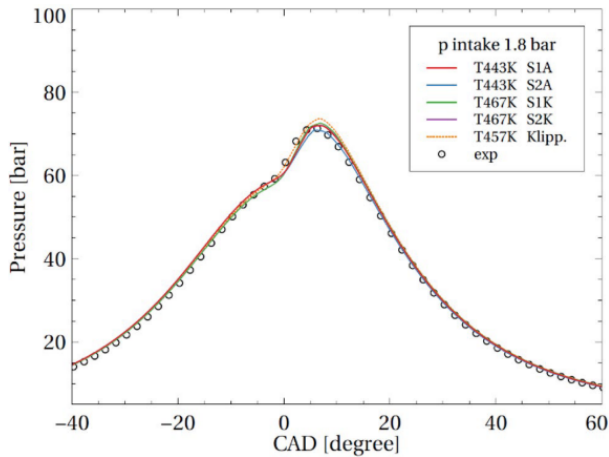


Figure 5.15: Calibrated pressure trace by means of inlet temperature for several MeOH kinetic models.

5.5 Combustion analysis of single and double injection strategy

Double injection strategies were investigated in an optical engine setup in the experimental work of Lönn [108]. Results show a significant reduction of the inlet temperature require-

ment for the double injection cases compared to the single injection cases, i.e., 47K. Optical experiments also show that the ignition kernel is located quite close to the injector nozzle, which in the next step, propagates downstream towards already injected fuel. The LES-PaSR approach was employed to investigate the mixing, ignition mechanism, and mode of combustion in two selected cases, a single injection case, SOI -2.2, and double injection case, SOI -11.2/-2.2, Paper V.

An acceptable agreement between the simulated and the experimental pressure trace was achieved by calibration of the intake temperature. PaSR approach was needed to improve the prediction of the fuel consumption rate.

Combustion mode analysis is performed with a qualitative method based on the distribution of the key species as oxygen, fuel, carbon monoxide and distribution of heat release rate. The employed method allows to distinguish between the premixed and non-premixed type of combustion. The presence of the premixed flame mode cannot be confirmed. An attempt to distinguish between the ignition mode and the flame mode, in similar PPC engine conditions for gasoline surrogate fuels, was recently performed by Ibrón et al. [116]. The budget term method in LES framework was used, which implied that the dominant mode of combustion is the ignition front propagation mode rather than flame propagation mode. DNS studies for dual-fuel combustion, including methanol, by Hu et al. [128] also imply an ignition dominant combustion. Thereby, it is expected that the dominant mode of combustion in methanol PPC engines is the ignition mode. In addition, methanol as an oxygenated fuel, may perform differently under the non-premixed combustion mode, compared with gasoline or diesel. Thus, it is still of interest to investigate the local transition between the ignition mode and non-premixed mode. Figure 5.18 and Figure 5.19 show the corresponding pressure traces and comparison of natural luminosity with temperature field at CA50 to validate combustion behavior, see Paper V.

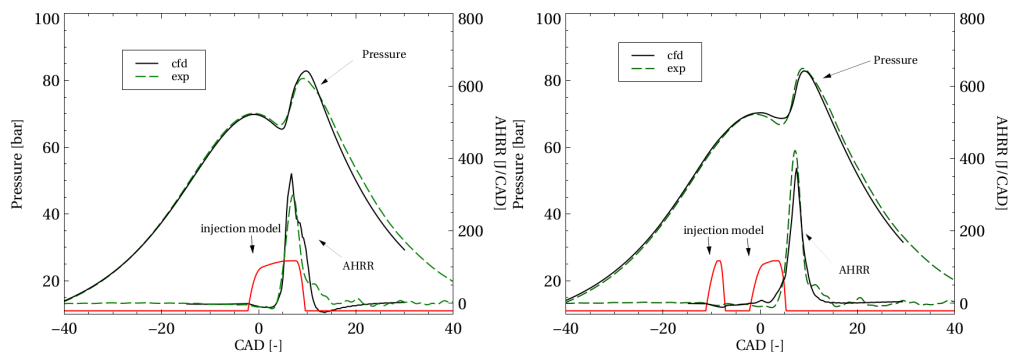


Figure 5.16: Pressure trace SOI-2.2 (left column) and SOI-11.2/-2.2 (right column).

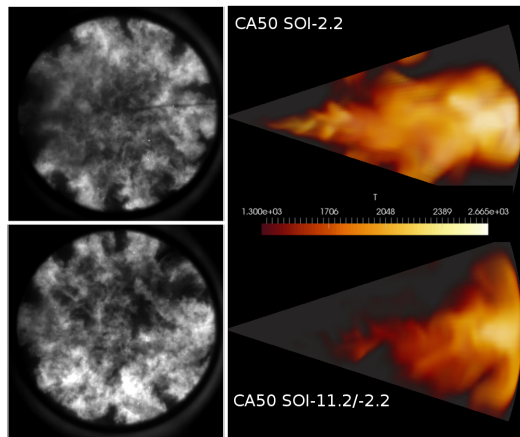


Figure 5.17: Natural luminosity (left) and numerical temperature field (right).

The combustion cycle can be divided into three phases. The first phase is the lean premixed combustion, where ignition kernel is formed around $0.2 < \phi < 0.4$ and the reaction zone starts to propagate towards the richer conditions. The second phase is the rich premixed phase, where reaction front crosses the stoichiometry line and consume premixed fuel rich mixtures. The third phase is the diffusion flame mode phase, which is caused by the deficit of the oxygen within the fuel rich conditions. The diffusion flame is located at the stoichiometry line, where unburned fuel that has originated from the fuel rich side, can oxidize and react with the remaining oxygen located on the lean side. Figures 5.18 and 5.19 show spatial distribution of fuel, carbon monoxide, heat release rate and oxygen for each combustion phase, for the single and double injection case, respectively. The effect of pilot injection in assisting the ignition of the main fuel is captured well. The onset of ignition starts at the location of the pilot fuel, which is also confirmed by the fuel tracking method.

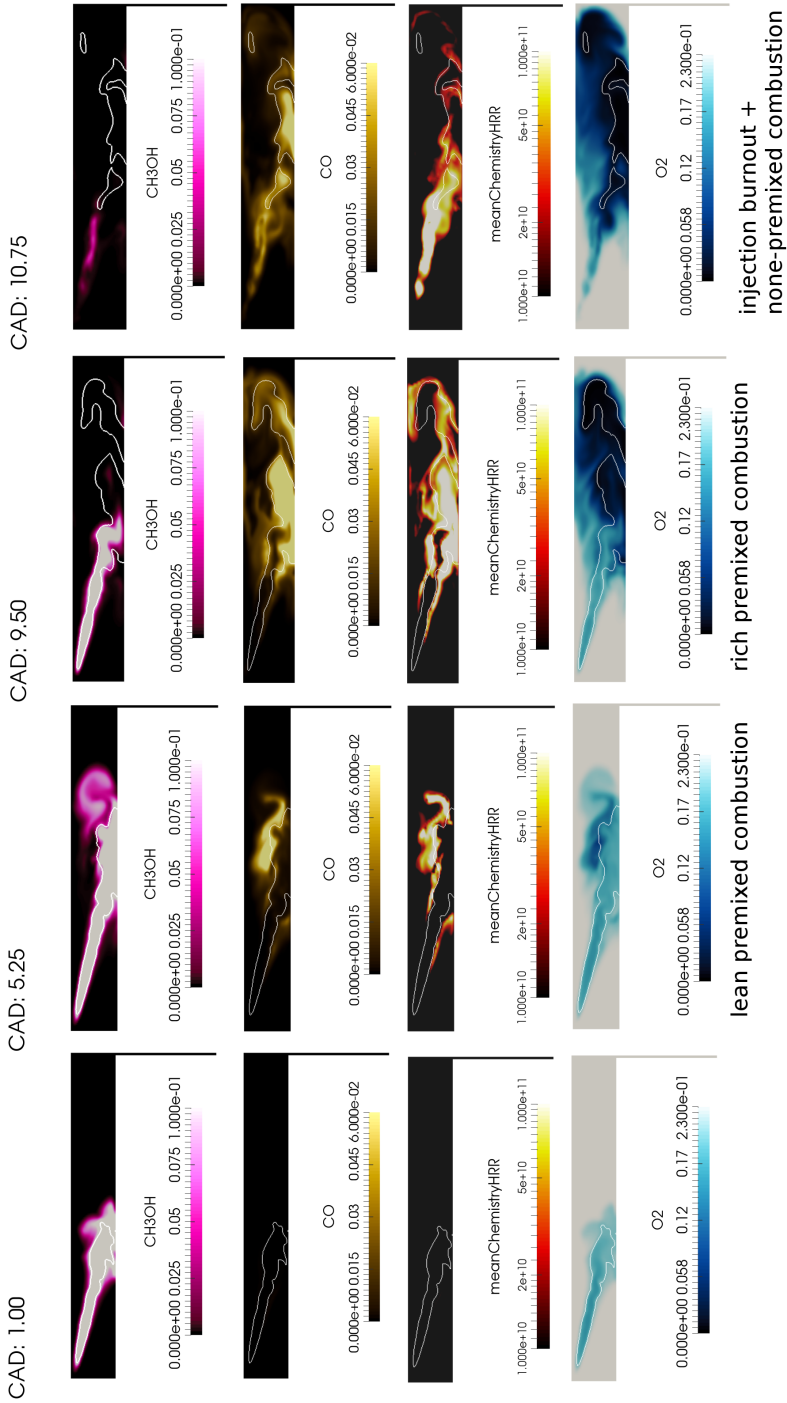


Figure 5.18: Ignition sequence and combustion mode analysis based on the key species CH₃OH, CO, O₂ and distribution of HRR for the single injection case SOI -2.2. Solid white line shows $\phi = 1$.

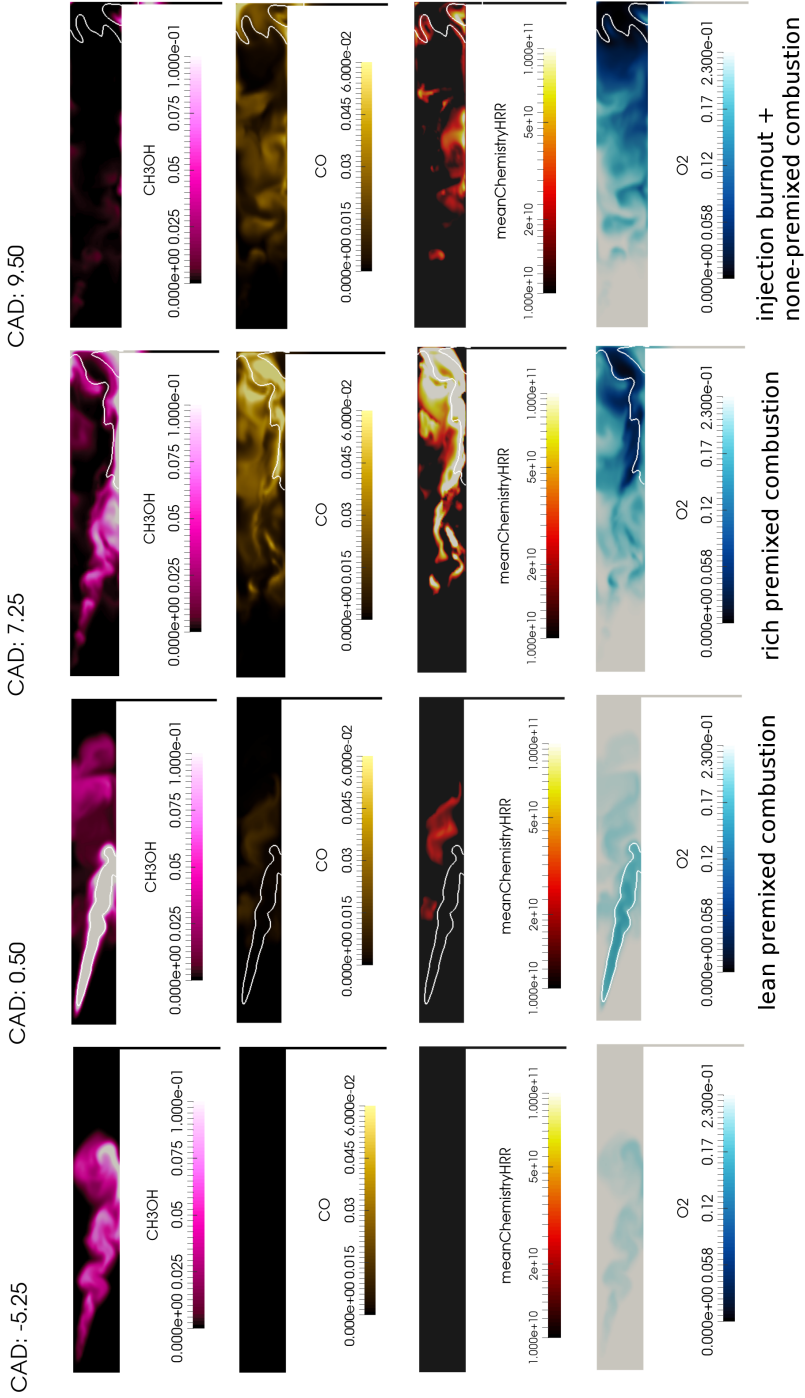


Figure 5.19: Ignition sequence and combustion mode analysis based on the key species CH₃OH, CO, O₂ and distribution of HRR for the double injection case SOI -11.2/-2.2. Solid white line shows $\phi = 1$.

Both injection cases resulted in fuel lean and fuel rich mixtures, leading to a combination of premixed and none-premixed combustion modes i.e., partially premixed combustion. However, depending on the distribution of the heat release between the lean, the stoichiometric, and the rich mixtures, the average combustion temperature is different, which will lead to differences in the engine performance. Figure 5.20 shows the allocation of the total heat release during each combustion phase. The total heat release in the double injection case is shifted towards leaner conditions, including less stoichiometric mixtures, which reduces emission of NO_x and wall heat losses. The single injection case includes more stoichiometric mixtures giving higher combustion temperature and better conversion of HC and CO.

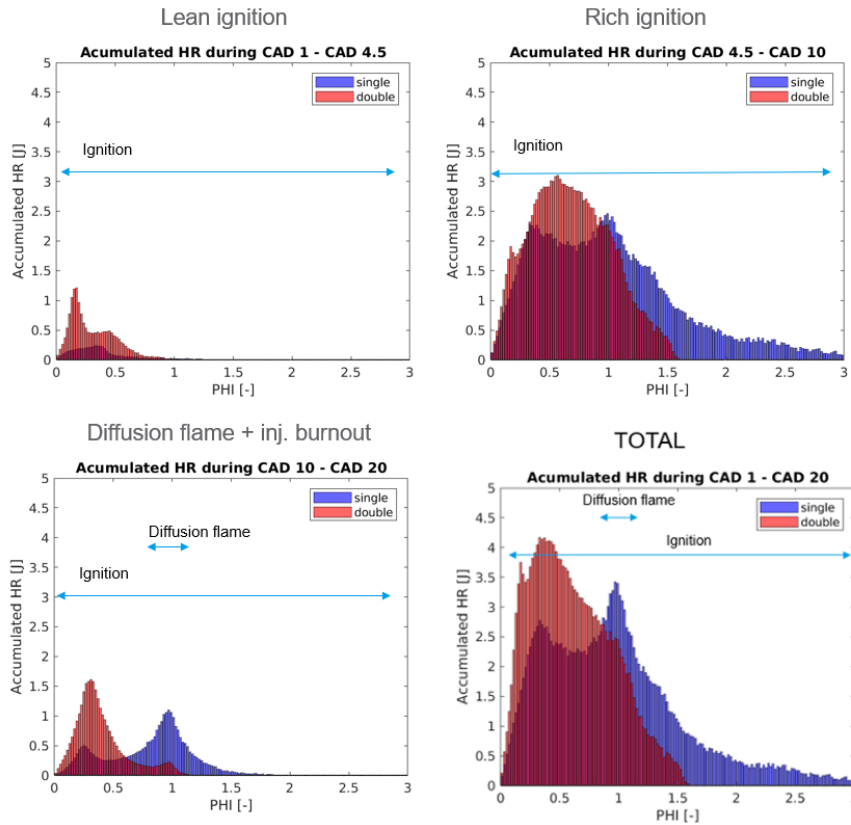


Figure 5.20: Allocation of heat release with respect to Φ during combustion cycle for SOI -2.2 and SOI -11.2/-2.2.

5.6 Transient liquid penetration length

Methanol liquid penetration lengths are investigated in optical engine experiments and used to validate spray modeling. A common practice in the spray calibration process is to change the droplet brake-up time scale, $B1$ [72]. The initial droplet size distribution is presumed with the Rosin-Rammler distribution. The liquid spray validation is based on the injection case SOI -25 and SOI -8 aTDC. Figure 5.22 shows instantaneous snapshots of Mie-scattering measurement and LES at the half of the injection time. Transient liquid penetration length is presented in Figure 5.21. It is worth noticing that the injection delay between the current signal to the injector and the physical injection of the droplets into the domain is about 3 CAD. This delay is considered in the simulations. Acceptable agreement was achieved with KH-RT break-up model by setting $B1 = 6$. Target grid size for both cases is 0.25 mm with the total number of parcel set to 100,000.

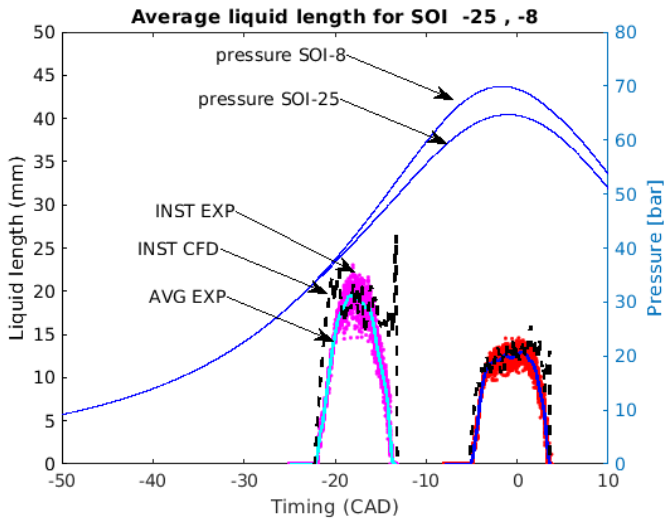


Figure 5.21: Methanol transient liquid penetration length. Initial conditions: $T=343\text{K}$, $P=1.5\text{ bar}$, $\text{injDuration}=900\mu\text{s}$, $\text{CR}=16$. Alex Matamis is acknowledged for post-processing optical data.

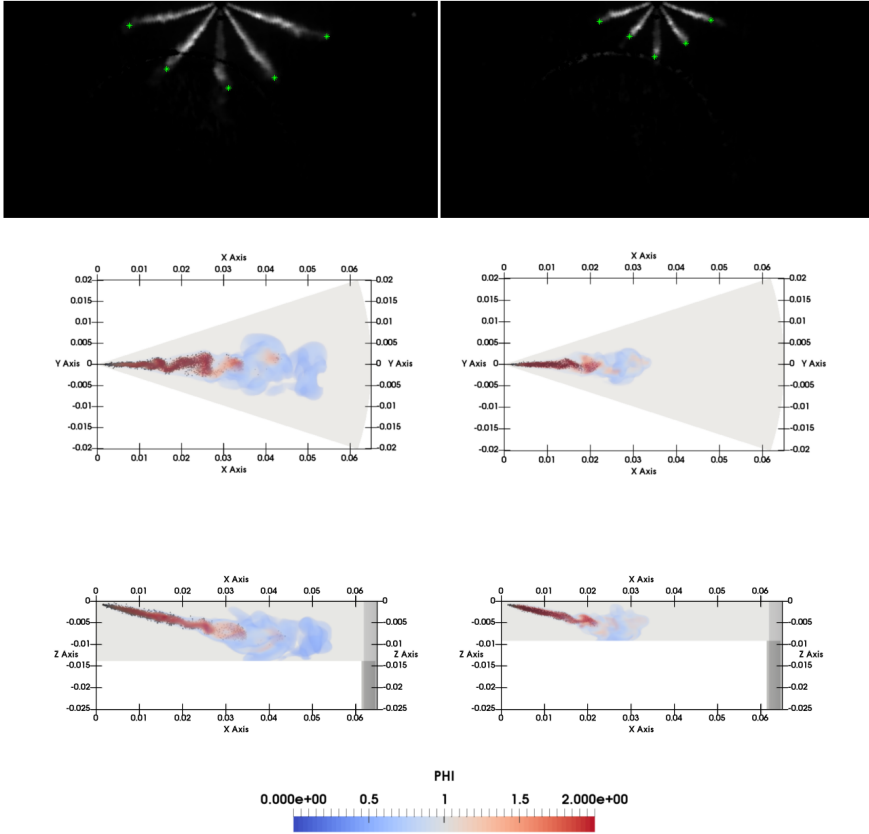


Figure 5.22: Methanol liquid spray Mie-scattering measurements (top row) SOI -25 and SOI -8. CFD snapshots at the half of the injection time presenting parcels and vapor (two bottom rows). Initial conditions: $T=343\text{K}$, $P=1.5\text{ bar}$, $\text{injDuration}=900\mu\text{s}$, $\text{CR}=16$. Alex Matamis is acknowledged for providing optical data.

Chapter 6

Results and discussion: diesel spray - wall interaction

This chapter presents numerical results for the diesel impingement studies. The focus is set on the air entrainment mechanisms and the consequences on the soot oxidation process.

6.1 Influence of wall position

LES was employed to study mixing mechanisms in the impingement diesel sprays. In the experimental work of Li et al. [129, 130], soot emissions were investigated with optical tools by calculation of soot absorption factor, KL [112]. It was found that during the injection time, the wall jet cases resulted in a somewhat higher instantaneous KL compared to the free jet configuration. However, after the end of injection, the decay of KL showed to be faster and thus it is considered that the wall impingement had a positive effect on the soot oxidation process. Motivated by the experimental observation, the goal is to investigate the underlying mixing mechanisms governing the air entrainment into the spray plume which are 1) flame lift-off length, 2) impingement enhanced mixing and 3) entrainment wave [53]. The goal is to understand how the effect of the wall changes the importance of each mechanism and what are the consequences on the oxidation of soot.

The time sequence of temperature field is shown in Figure 6.1. One can observe that the onset of ignition is taking place before the fuel vapor makes contact with the wall (30 mm case) leading to more premixed charge at the onset of ignition. Due to the short distance, the impingement bulk velocity is higher, which will create more turbulence and as a result more mixing caused by the impingement vortices compared to 50 mm case. The position and size of impingement vortices will have a strong effect on enhancing the mixing.

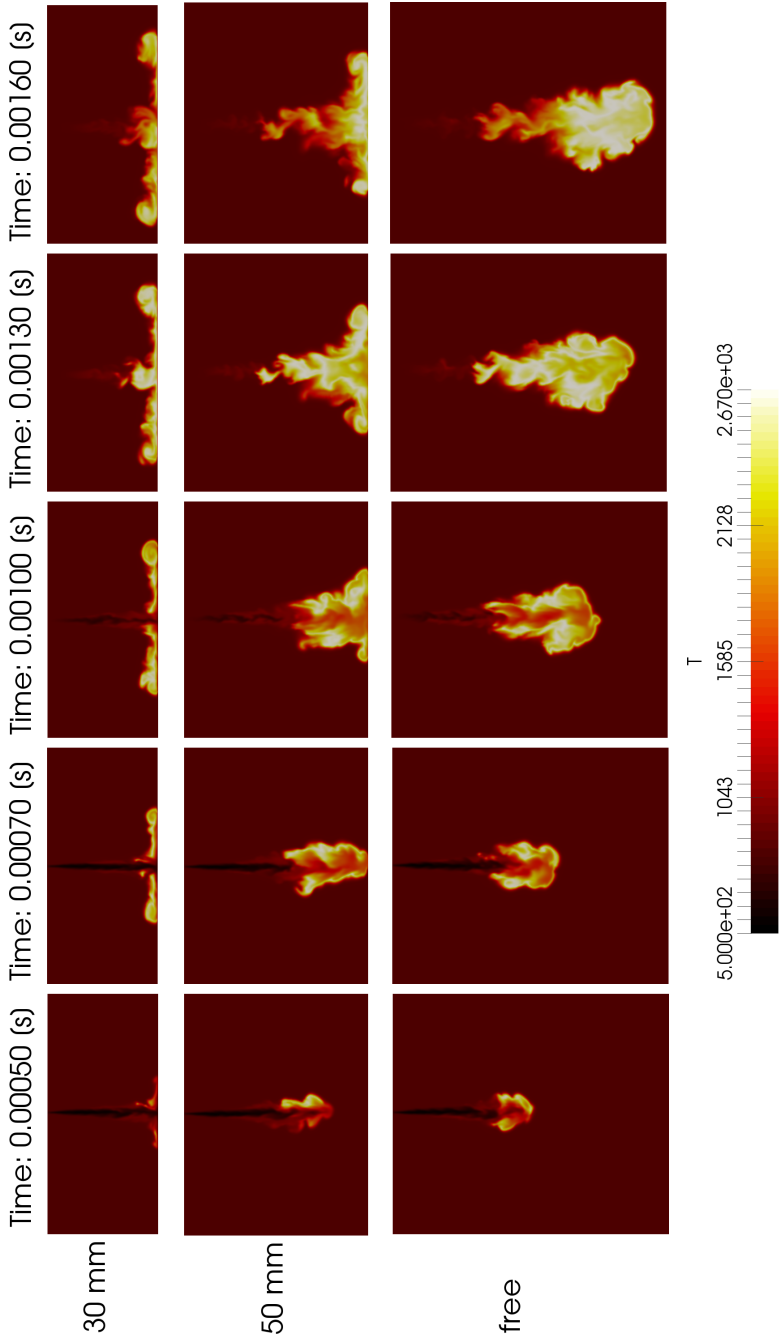


Figure 6.1: Time sequence of the temperature distribution in a 2D-plane for 30 mm, 50 mm and free jet cases.

The validation is based on the comparison between a numerical and experimental line-of-sight, OH^* chemiluminescence. A numerical line-of-sight is calculated using the volumetric average. Since the chemical kinetic mechanism lacks OH^* that could be directly compared to the experimental data, a product of numerical $\text{OH} \times \text{CO}$ is used instead, following suggestions in Refs. [131–133]. Figure 6.2 shows that simulations correspond well to the position and the intensity of the reaction zone observed in the experiments. The wall jet case with 50 mm distance to the wall, shows the highest intensity signal in the near wall region, which is captured in the simulations.

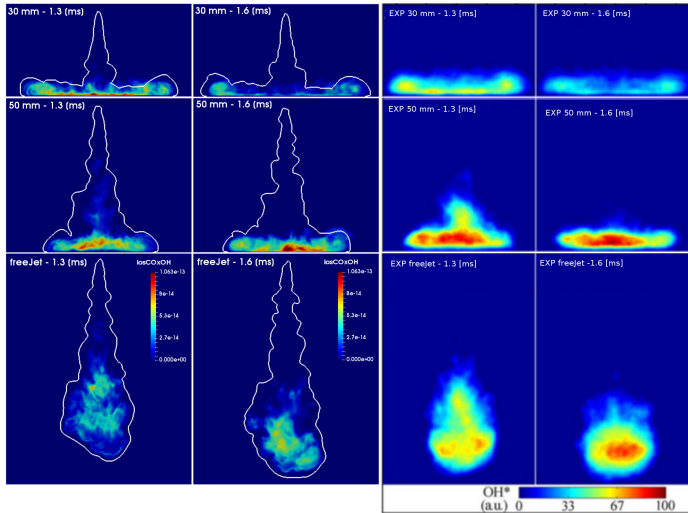


Figure 6.2: Comparison of numerical line-of-sight $\text{OH} \times \text{CO}$ (two left columns) and experimental line-of sight OH^* (two right columns) at 1.3 ms and 1.6 ms aSOI.

It is hypothesized that, at the time of the maximized soot formation, i.e., 0.8 ms after SOI, the impingement flow in the 50 mm case, promotes the soot formation. The soot formation can be enhanced by the wall blocking effect in the impingement region, where mixtures, at which soot is formed ($1600\text{K} < T < 2200\text{K}$, $\phi > 2$), are accumulated. The impingement vortices in the 50 mm case, during the soot formation time, are not yet developed in order to enhance the mixing, whereas in the 30 mm case, the impingement vortices can already improve the mixing process. Figure 6.3 shows the region of the soot formation, identified by ($1600\text{K} < T < 2200\text{K}$, $\phi > 2$) and the corresponding soot formation region modeled with the employed soot model [134]. Figure 6.4 shows the experimental distribution of KL and numerical equivalent of volume averaged numerical soot volume fraction. In these figures, the 50 mm wall jet case resulted in the soot formation located in a compact near wall region.

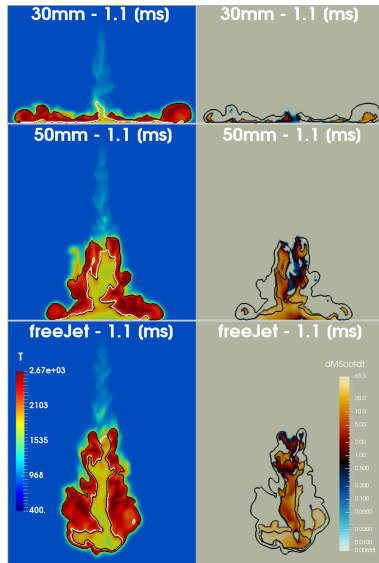


Figure 6.3: Soot formation region represented by $T - \phi$ manifold (left column) with $\phi = 2$ (white line) and $T = 2200K$ (black line) and modeled soot formation rate (right column).

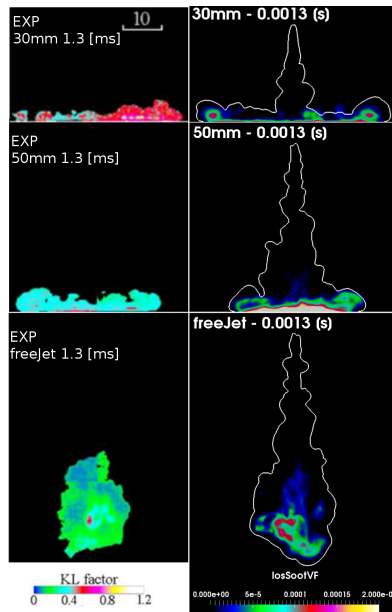


Figure 6.4: Experimental line-of-sight KL (left column) and numerical equivalent line-of-sight of modeled sootVF (right column). The solid white line indicates spray boundary $Z=0.01$.

The soot formation in the 30 mm case is distributed in a thin layer, which is also located within the impingement vorticies. The soot formation in the free jet case is located within the spray head. It is noteworthy, that the average temperature in the free jet case should be higher due to the lack of the wall cooling effect ($T_{wall} = 873K$) and thus more mass can achieve temperatures, outside of the soot formation range. Whereas, the gas temperatures in the wall jet cases, may be located closer to the formation temperature range. On the other hand, due to the enhanced mixing, wall jet cases may result, in leaner conditions which are outside of the equivalence ratio condition for the soot formation, i.e., $\phi > 2$. The focus is set on the air entrainment rate.

The air entrainment rate into the spray plume is calculated based on the mixture fraction Z with the following expression:

$$\frac{dm_a}{dt} = (1 - Z)m_{tot} \quad (6.1)$$

where m_a is mass of the air and m_{tot} is the total mass of the spray vapor. Figure 6.5 shows the air entrainment rate, whereas Figure 6.6 show the flame lift-off length.

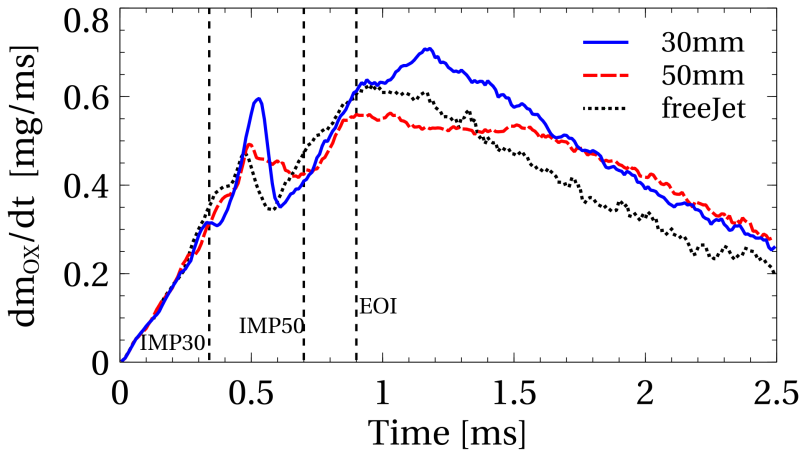


Figure 6.5: Air entrainment rate.

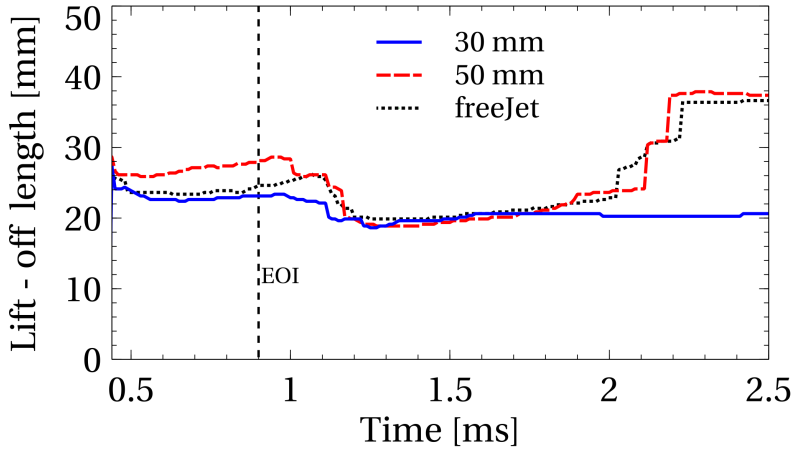


Figure 6.6: Flame lift-off length.

The distribution of oxygen is presented in Figure 6.7. By analyzing the direction from which oxygen penetrates into the low oxygen regions, one can qualitatively judge which mixing mechanism is acting. In the free jet case, one can note that oxygen is entrained from the tail of the spray plume at a faster rate, compared to the mixing which takes place in the leading front of the spray head. This phenomenon is similar to that discussed by Musculus and referred to as the entrainment wave [53]. The mixing mechanism in the wall jet cases is enhanced by the wall impingement. As it can be observed in Figure 6.5, the 30 mm wall jet resulted in a "mixing boost" just after the EOI, meaning that both mixing mechanisms, which are the entrainment wave and the impingement mixing, act together during a short time. In the 50 mm case, these two mechanisms act in a sequence, and results in a constant air entrainment rate during a longer period of time, which eventually gives more total entrained air, compared with the free jet case. Figure 6.7, at 2.1 ms aSOI, shows that the low mass fraction region of oxygen is relatively small for the wall jet cases, whereas for the free jet case, the low oxygen region remains, mostly within the spray head at possible location of soot. Thus, it can be considered that due to the better air entrainment rate in both wall jet cases after the EOI, the oxidation process of soot is faster in comparison to the free jet case, which is in the agreement with the experimental work of Li et al. [129, 130].

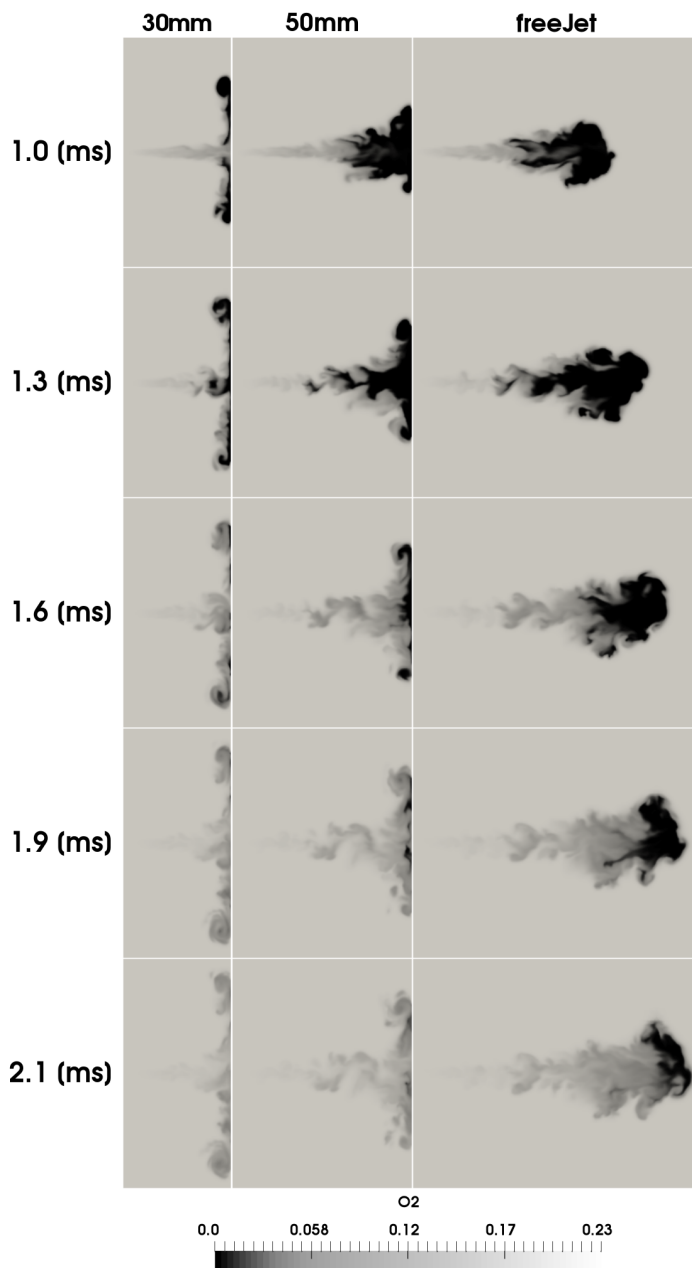


Figure 6.7: Time sequence of oxygen (O_2) mass fraction after the end of injection (EOI). Regions of low oxygen concentration suggests possible soot regions.

Chapter 7

Summary

7.1 Concluding remarks

Methanol PPC can be achieved at quite late injection timings (similar to those in diesel engines), compared for example, to gasoline. The reason is the low stoichiometric air to fuel ratio ($A/F_s = 6.47$). The advanced injections between SOI -30 and SOI -5 without EGR, results in the HCCI like combustion, i.e., all fuel lean mixtures. Late injection times for methanol PPC can ease targeting of the fuel injection to inside of the piston bowl, which can reduce the losses associated with the crevice volumes and utilize a stronger interaction with the piston bowl shape. The non-sooting combustion of methanol allows burning in the mixing controlled mode if needed, only at the cost of higher NO_x emissions. Late injection timings are also beneficial for the reduction of the gas exchange losses. Mixing controlled combustion needs to be employed especially, at higher loads, to reduce the rapid pressure rise rate caused by the premixed burn. The main disadvantage of methanol compression ignition is the high intake temperature requirement, which is caused by the high latent heat of vaporization. Improvements can be made by employing multiple injection strategies, glow plugs, or optimizing engine compression ratio.

The CFD modeling of methanol PPC engines and in general the PPC engine concept has shown to be challenging due to the potential existence of all fundamental combustion modes as ignition front propagation, premixed flame propagation, and non-premixed flame. In this work, focus was set on distinguishing between the premixed and non-premixed combustion modes. The RANS-WSR approach gives reasonable prediction in low stratified conditions $0.2 < \phi < 0.5$. Highly stratified cases $0.2 < \phi < 2.5$, i.e., including local rich mixtures, are largely over-predicted by RANS-WSR. Such cases in this thesis were improved by employing PaSR approach. The PaSR approach, based on gained experience, is rather an empirical approach since it needs calibration of a model constant that works for a narrow range of conditions. It does not provide a better prediction ability across the full range of SOIs. PPC studies in the literature with more advanced models i.e., transported

PDF approach, showed better prediction ability, but at much higher cost.

The ignition sequence of methanol at all tested conditions starts at nearly the leanest mixtures, $0.25 < \phi < 0.3$. The reason behind this is most likely the cooling effect of methanol that prevents the auto-ignition event. The ignitable methanol vapor is more sensitive to the temperature rather than the equivalence ratio, meaning that the onset of ignition will occur at locations where methanol can quickly heat-up by mixing with the hot ambient air. Fast mixing and heating of methanol vapor is located at high turbulent regions, such as spray shear layer or spray-wall interaction regions. In the optical work of Lönn et al. [108], the onset of ignition occurred close to the injector nozzle.

The categorization of PPC engines is not consistent. It depends on the undefined mixture composition that during combustion would result in the "sweet-spot" in the emissions trade-off between the HC/CO and NO_x . Additionally, the stratified mixture composition may or may not include locally rich mixtures to achieve that. Presence of locally fuel rich mixtures leads to the diffusion combustion mode. The practical operation of PPC engines seems to include both scenarios, depending on the load and EGR content needed. Low load cases, regardless of very late SOIs, may result in all fuel lean mixtures, burning as a "stratified HCCI". Higher load cases will start to include local rich mixtures, giving rise to combination of the premixed mode burn and the none-premixed mode burn, i.e., PPC.

Diesel impingement sprays in the optical experiments of Li et al. [129, 130] imply that the soot oxidation can be improved due to the wall interaction. LES studies showed that underlying mechanisms for the air entrainment which are flame lift-off length, impingement enhanced mixing, and Musculus's entrainment wave changes due to the wall interaction. Regardless of temporary "wall blocking effect" for the 50 mm wall case, the oxidation process seems to be faster for both wall jet configurations (30 mm and 50 mm), especially after the end of injection. This result does not yield that wall impingement always improves soot oxidation. Other parameters such as wall temperature, injection pressure, wall curvature, injection duration, EGR content as well as double injection strategies may have a strong impact.

7.2 Future work

Based on the performed simulations interesting aspects worth of further consideration are listed as follows:

- Investigated piston bowl designs should be further developed and tested in a real engine setup based on the target range of start of injection. The recommended piston bowl shape for methanol PPC is the double step piston.
- In order to improve calibration process of intake temperature in simulations, it can be of great use to measure the in-cylinder temperature in a motored cycle at TDC position. An additional reference temperature point would help to validate the predicted temperature at TDC, which is essential for prediction of ignition kernel.
- Due to the existence of multi combustion modes in PPC engines, the CFD simulations have been based on the directly coupling with the finite rate chemistry. This method is time consuming and therefore more efficient CFD models, e.g., based on tabulation, should be further developed and tested.
- Impingement diesel spray studies should be continued with double injection strategies to investigate the air entrainment rate and soot oxidation in more realistic injection scenarios.

Bibliography

- [1] World Health Organization. “Ambient Air Pollution: A global assessment of exposure and burden of disease”. In: *World Heal. Organ.* (2016), pp. 1–131.
- [2] International Energy Agency (IEA). “CO2 Emissions from Fuel Combustion 2018 Highlights”. In: *Int. energy agency* 1.1 (2018).
- [3] Johannes Kester et al. “Policy mechanisms to accelerate electric vehicle adoption: A qualitative review from the Nordic region”. In: *Renew. Sustain. Energy Rev.* 94 (2018), pp. 719–731.
- [4] I López et al. “Next generation electric drives for HEV/EV propulsion systems: Technology, trends and challenges”. In: *Renew. Sustain. Energy Rev.* 114 (2019), p. 109336.
- [5] Debora Fino et al. “A review on the catalytic combustion of soot in Diesel particulate filters for automotive applications: From powder catalysts to structured reactors”. In: *Appl. Catal. A Gen.* 509 (2016), pp. 75–96.
- [6] M. Shelef. “Selective Catalytic Reduction of NO_x with N-Free Reductants”. In: *Chem. Rev.* 95.1 (1995), pp. 209–225.
- [7] John E. Dec. “Advanced compression-ignition engines - Understanding the in-cylinder processes”. In: *Proc. Combust. Inst.* 32 II.2 (2009), pp. 2727–2742.
- [8] Mark P.B. Musculus, Paul C. Miles, and Lyle M. Pickett. *Conceptual models for partially premixed low-temperature diesel combustion*. Vol. 39. 2-3. Progress in Energy and Combustion Science, 2013, pp. 246–283.
- [9] Takeyuki Kamimoto and Myurng Hoan Bae. “High combustion temperature for the reduction of particulate in diesel engines”. In: *SAE Tech. Pap.* SAE International, 1988.
- [10] Henrik Nordgren, Anders Hultqvist, and Bengt Johansson. “Start of injection strategies for HCCI-combustion”. In: *SAE Tech. Pap.* 2004.
- [11] Vittorio Manente, Bengt Johansson, and Per Tunestal. “Partially Premixed Combustion at High Load using Gasoline and Ethanol, a Comparison with Diesel”. In: (2009).

- [12] Vittorio Manente. *Gasoline Partially Premixed Combustion An Advanced Internal Combustion Engine Concept Aimed to High Efficiency, Low Emissions and Low Acoustic Noise in the Whole Load Range*. 2010.
- [13] Vittorio Manente et al. "Effects of Ethanol and Different Type of Gasoline Fuels on Partially Premixed Combustion from Low to High Load". In: *SAE Int. 2010-01-0871* (2010).
- [14] Gautam T. Kalghatgi, Per Risberg, and Hans-Erik Angstrom. "Partially Pre-Mixed Auto-Ignition of Gasoline to Attain Low Smoke and Low NO_x at High Load in a Compression Ignition Engine and Comparison with a Diesel Fuel". In: *SAE Tech. Pap. Ser. 1.724* (2010).
- [15] Mehrzad Kaiadi et al. "Sensitivity Analysis Study on Ethanol Partially Premixed Combustion". In: *SAE Int. J. Engines* 6.1 (2013), pp. 269–2013.
- [16] P. C. Bakker et al. "Characterization of low load PPC operation using RON70 fuels". In: *SAE Tech. Pap.* Vol. 1. 2014.
- [17] Cornelis Havenith, Heinz Kuepper, and Ulrich Hilger. "Performance and emission characteristics of the deutz glow plug assisted heavy-duty methanol engine". In: *SAE Tech. Pap.* 1987.
- [18] Ganesh Duraisamy, Murugan Rangasamy, and Govindan Nagarajan. "Effect of EGR and Premixed Mass Percentage on Cycle to Cycle Variation of Methanol/Diesel Dual Fuel RCCI Combustion". In: *SAE Tech. Pap.* Vol. 2019-Janua. January. 2019.
- [19] Zhenkan Wang et al. "Simultaneous 36 kHz PLIF/chemiluminescence imaging of fuel, CH₂O and combustion in a PPC engine". In: *Proc. Combust. Inst.* 37.4 (2019), pp. 4751–4758.
- [20] Haifeng Liu et al. "A comparative study on partially premixed combustion (PPC) and reactivity controlled compression ignition (RCCI) in an optical engine". In: *Proc. Combust. Inst.* 37.4 (2019), pp. 4759–4766.
- [21] Zunqing Zheng et al. "Study on the flame development patterns and flame speeds from homogeneous charge to stratified charge by fueling n-heptane in an optical engine". In: *Combust. Flame* 199 (2019), pp. 213–229.
- [22] Marcus Lundgren et al. "Optical study on combustion transition from HCCI to PPC with gasoline compression ignition in a HD engine". In: *SAE Tech. Pap.* Vol. 2016-April. April. 2016.
- [23] Yanzhao An et al. "Analysis of Transition from HCCI to CI via PPC with Low Octane Gasoline Fuels Using Optical Diagnostics and Soot Particle Analysis". In: *SAE Tech. Pap.* Vol. 2017-October. 2017.
- [24] Christian Ibrón et al. "Effect of Injection Timing on the Ignition and Mode of Combustion in a HD PPC Engine Running Low Load". In: *SAE Tech. Pap. Ser.* Vol. 1. 2019.

- [25] Leilei Xu et al. “Combustion characteristics of gasoline DICl engine in the transition from HCCI to PPC: Experiment and numerical analysis”. In: *Energy* 185 (2019), pp. 922–937.
- [26] Changle Li et al. “Effect of Piston Geometry on Stratification Formation in the Transition from HCCI to PPC”. In: *SAE Tech. Pap.* Vol. 2018-Septe. 2018.
- [27] Sebastian Verhelst et al. “Methanol as a fuel for internal combustion engines”. In: *Prog. Energy Combust. Sci.* 70 (2019), pp. 43–88.
- [28] Sam Shamun et al. “Detailed characterization of particulate matter in alcohol exhaust emissions”. In: *COMODIA 2017 - 9th Int. Conf. Model. Diagnostics Advanved Engine Syst.* (2017).
- [29] Sam Shamun et al. “Exhaust PM Emissions Analysis of Alcohol Fueled Heavy-Duty Engine Utilizing PPC”. In: *SAE Int. J. Engines* 9.4 (2016), pp. 2016–01–2288.
- [30] Erik Svensson et al. “Potential Levels of Soot, NO_x, HC and CO for Methanol Combustion”. In: *SAE Tech. Pap. 2016-01-0887* 2016-April (2016).
- [31] Sam Shamun et al. “Experimental investigation of methanol compression ignition in a high compression ratio HD engine using a Box-Behnken design”. In: *Fuel* 209 (2017), pp. 624–633.
- [32] Erik Svensson et al. “Combined Low and High Pressure EGR for Higher Brake Efficiency with Partially Premixed Combustion”. In: *SAE Tech. Pap.* Vol. 2017-October. 2017.
- [33] Erik Svensson, Martin Tuner, and Sebastian Verhelst. “Influence of Injection Strategies on Engine Efficiency for a Methanol PPC Engine”. In: *SAE Tech. Pap. Ser.* Vol. 1. 2019.
- [34] J. B. Heywood. *Internal combustion engine fundamentals, volume 930*. McGraw-Hill, 1988, p. 930.
- [35] Norbert Peters. *Turbulent Combustion*. Cambridge Monographs on Mechanics. Cambridge University Press, 2000.
- [36] R. W. Bilger et al. “Paradigms in turbulent combustion research”. In: *Proc. Combust. Inst.* 30.1 (2005), pp. 21–42.
- [37] Ya B. Zeldovich. “Regime classification of an exothermic reaction with nonuniform initial conditions”. In: *Combust. Flame* 39.2 (1980), pp. 211–214.
- [38] Ankit Bhagatwala et al. “Numerical investigation of spontaneous flame propagation under RCCI conditions”. In: *Combust. Flame* 162.9 (2015), pp. 3412–3426.
- [39] Seung Ook Kim et al. “A DNS study of the ignition of lean PRF/air mixtures with temperature inhomogeneities under high pressure and intermediate temperature”. In: *Combust. Flame* 162.3 (2015), pp. 717–726.

- [40] F. Zhang, R. Yu, and X.S. Bai. “Direct numerical simulation of PRF70/air partially premixed combustion under IC engine conditions”. In: *Proc. Combust. Inst.* 35.3 (2015), pp. 2975–2982.
- [41] F. Zhang et al. “Direct numerical simulation of flame/spontaneous ignition interaction fueled with hydrogen under SACI engine conditions”. In: *Int. J. Hydrogen Energy* 42.6 (2017), pp. 3842–3852.
- [42] M. Jangi et al. “Modelling of Methanol Combustion in a Direct Injection Compression Ignition Engine using an Accelerated Stochastic Fields Method”. In: *Energy Procedia* 105 (2017), pp. 1326–1331.
- [43] Jery Chomiak and Anders Karlsson. “Flame liftoff in diesel sprays”. In: *Symp. Combust.* 26.2 (1996), pp. 2557–2564.
- [44] B. F. Magnussen and B. H. Hjertager. “On mathematical modeling of turbulent combustion with special emphasis on soot formation and combustion”. In: *Symp. Combust.* 16.1 (1977), pp. 719–729.
- [45] C Felsch et al. “Applying Representative Interactive Flamelets (RIF) with Special Emphasis on Pollutant Formation to Simulate a DI Diesel Engine with Roof-Shaped Combustion Chamber and Tumble Charge Motion”. In: *SAE Tech. Pap.* 2007-01-0167 2007.724 (2007), pp. 776–790.
- [46] Ulaş Egüz et al. “Modeling of PCCI combustion with FGM tabulated chemistry”. In: *Fuel* 118 (2014), pp. 91–99.
- [47] Armin Wehrfritz et al. “Large Eddy Simulation of n-dodecane spray flames using Flamelet Generated Manifolds”. In: *Combust. Flame* 167 (2016), pp. 113–131.
- [48] T. Lucchini et al. “Modeling advanced combustion modes in compression ignition engines with tabulated kinetics”. In: *Appl. Energy* 247 (2019), pp. 537–548.
- [49] Amin Maghbouli et al. “Modelling compression ignition engines by incorporation of the flamelet generated manifolds combustion closure”. In: *Combust. Theory Model.* 23.3 (2019), pp. 414–438.
- [50] Marcus Lundgren. “Optical Diagnostics of Gasoline Compression Ignition : HCCI-PPC-Diffusion Combustion”. PhD thesis. Lund University, 2017, p. 195.
- [51] John E. Dec. “A conceptual model of di diesel combustion based on laser-sheet imaging”. In: *SAE Tech. Pap.* 1997.
- [52] Dennis L. Siebers. “Scaling liquid-phase fuel penetration in diesel sprays based on mixing-limited vaporization”. In: *SAE Tech. Pap.* 1999.
- [53] Mark P.B. Musculus. “Entrainment waves in decelerating transient turbulent jets”. In: *J. Fluid Mech.* 638 (2009), pp. 117–140.
- [54] Lyle M. Pickett and J. Javier López. “Jet-wall interaction effects on diesel combustion and soot formation”. In: *SAE Tech. Pap.* 2005.724 (2005).

- [55] Gilles Bruneaux. "Mixing process in high pressure diesel jets by normalized laser induced exciplex fluorescence part I: Free jet". In: *SAE Tech. Pap.* c (2005).
- [56] G. Bruneaux. "Combustion structure of free and wall-impinging diesel jets by simultaneous laser-induced fluorescence of formaldehyde, poly-aromatic hydrocarbons, and hydroxides". In: *Int. J. Engine Res.* 9.3 (2008), pp. 249–265.
- [57] Gilles Bruneaux, Mickael Causse, and Alaa Omrane. "Air entrainment in Diesel-like gas jet by simultaneous flow velocity and fuel concentration measurements, comparison of free and wall impinging jet configurations". In: *SAE Int. J. Engines* 5.2 (2012), pp. 76–93.
- [58] Noud Maes et al. "Heavy-Duty Diesel Engine Spray Combustion Processes: Experiments and Numerical Simulations". In: *SAE Tech. Pap.* Vol. 2018-Sept. 2018.
- [59] Ahmad Hadadpour, Mehdi Jangi, and Xue Song Bai. "Jet-jet interaction in multiple injections: A large-eddy simulation study". In: *Fuel* 234. July (2018), pp. 286–295.
- [60] Ahmad Hadadpour et al. "The role of a split injection strategy in the mixture formation and combustion of diesel spray: A large-eddy simulation". In: *Proc. Combust. Inst.* 37.4 (2019), pp. 4709–4716.
- [61] Noud Maes. "The life of a spray". PhD thesis. Department of Mechanical Engineering, 2019.
- [62] Tankai Zhang et al. "Effects of a wave-shaped piston bowl geometry on the performance of heavy duty Diesel engines fueled with alcohols and biodiesel blends". In: *Renew. Energy* (2019).
- [63] Kenan Muric, Per Tunestal, and Ingemar Magnusson. "Medium and high load performance of partially premixed combustion in a wave-piston multi-cylinder engine with diesel and PRF70 fuel". In: *ASME 2018 Intern. Combust. Engine Div. Fall Tech. Conf. ICEF 2018*. Vol. 1. American Society of Mechanical Engineers, 2018.
- [64] Jan Eismark et al. "Role of Piston Bowl Shape to Enhance Late-Cycle Soot Oxidation in Low-Swirl Diesel Combustion". In: *SAE Int. J. Engines* 12.3 (2019), pp. 03–12–03–0017.
- [65] Jan Eismark et al. "Role of fuel properties and piston shape in influencing soot oxidation in heavy-duty low swirl diesel engine combustion". In: *Fuel* 254 (2019), p. 115568.
- [66] François G. Schmitt. "About Boussinesq's turbulent viscosity hypothesis: historical remarks and a direct evaluation of its validity". In: *Comptes Rendus - Mec.* 335.9-10 (2007), pp. 617–627.
- [67] S. E. Elghobashi and T. W. Abou-Arab. "A two-equation turbulence model for two-phase flows". In: *Phys. Fluids* 26.4 (1983), pp. 931–938.

- [68] Mehdi Jangi et al. “On large eddy simulation of diesel spray for internal combustion engines”. In: *Int. J. Heat Fluid Flow* 53 (2015), pp. 68–80.
- [69] K. Sone and S. Menon. “Effect of Subgrid Modeling on the In-Cylinder Unsteady Mixing Process in a Direct Injection Engine”. In: *J. Eng. Gas Turbines Power* 125.2 (2003), p. 435.
- [70] Thommie Nilsson et al. “Structures of turbulent premixed flames in the high Karlovitz number regime – DNS analysis”. In: *Fuel* 216 (2018), pp. 627–638.
- [71] S R Turns. *An introduction to combustion: concepts and applications*. Vol. 499. McGraw-Hill, 2000, p. 411.
- [72] Chen Huang and Andrei Lipatnikov. “Modelling of Gasoline and Ethanol Hollow-Cone Sprays Using OpenFOAM”. In: *SAE Pap.* (2011), pp. 327–344.
- [73] Rolf D. Reitz and Jennifer C. Beale. “Modeling Spray Atomization With the Kelvin-Helmholtz/Rayleigh-Taylor Hybrid Model”. In: *At. Sprays* 9.6 (1999), pp. 623–650.
- [74] W. RANZ. “Evaporation from drops 1”. In: *Chem. Engng. Prog.* 48 (1952), pp. 173–180.
- [75] Lyle M. Pickett et al. “Transient Rate of Injection Effects on Spray Development”. In: *SAE Int.* (2013), pp. 15–16.
- [76] Leilei Xu et al. “Experimental and modeling study of liquid fuel injection and combustion in diesel engines with a common rail injection system”. In: *Appl. Energy* 230 (2018), pp. 287–304.
- [77] Bassam S. E. Aljohani et al. “In Situ Injection Rate Measurement to Study Single and Split Injections in a Heavy-Duty Diesel Engine”. In: *SAE Tech. Pap. Ser.* 1 (2019), pp. 1–12.
- [78] Sibendu Som et al. “Comparison and standardization of numerical approaches for the prediction of non-reacting and reacting diesel sprays”. In: *SAE Tech. Pap.* 1 (2012).
- [79] Rickard Solsjö. “Mixing in Wall-Jets in a Heavy-Duty Diesel Engine : A LES Study”. In: *SAE Tech. Pap.* 2014-01-1127 (2009).
- [80] Vladimir Sabelnikov and Christer Fureby. “LES combustion modeling for high Re flames using a multi-phase analogy”. In: *Combust. Flame* 160.1 (2013), pp. 83–96.
- [81] Daniel Lörstad et al. “Experimental and les investigation of a SGT-800 burner in a combustion rig”. In: *Proc. ASME Turbo Expo*. Vol. 2. PARTS A AND B. ASMEDC, 2010, pp. 549–561.
- [82] Song Charng Kong and Rolf D. Reitz. “Numerical study of premixed HCCI engine combustion and its sensitivity to computational mesh and model uncertainties”. In: *Combust. Theory Model.* 7.2 (2003), pp. 417–433.

- [83] Tommaso Lucchini et al. “Towards the Use of Eulerian Field PDF Methods for Combustion Modeling in IC Engines”. In: *SAE Int. J. Engines 2014-01-1144* 7.1 (2014), pp. 286–296.
- [84] V. Raj Mohan and D. C. Haworth. “Turbulence-chemistry interactions in a heavy-duty compression-ignition engine”. In: *Proc. Combust. Inst.* 35.3 (2015), pp. 3053–3060.
- [85] Mehdi Jangi et al. “Effects of fuel cetane number on the structure of diesel spray combustion: An accelerated Eulerian stochastic fields method”. In: *Combust. Theory Model.* 19.5 (2015), pp. 549–567.
- [86] Mehdi Jangi et al. “Stabilization and liftoff length of a non-premixed methane/air jet flame discharging into a high-temperature environment: An accelerated transported PDF method”. In: *Combust. Flame* 162.2 (2015), pp. 408–419.
- [87] Mehdi Jangi, Mohammednoor Altarawneh, and Bogdan Z. Dlugogorski. “Large-eddy simulation of methanol pool fires using an accelerated stochastic fields method”. In: *Combust. Flame* 173 (2016), pp. 89–98.
- [88] Kar Mun Pang et al. “Modelling of diesel spray flames under engine-like conditions using an accelerated Eulerian Stochastic Field method”. In: *Combust. Flame* 193 (2018), pp. 363–383.
- [89] Mehdi Jangi and Xue Song Bai. “Multidimensional chemistry coordinate mapping approach for combustion modelling with finite-rate chemistry”. In: *Combust. Theory Model.* 16.6 (2012), pp. 1109–1132.
- [90] Mehdi Jangi et al. “Numerical Simulation of the ECN Spray A Using Multidimensional Chemistry Coordinate Mapping: n-Dodecane Diesel Combustion”. In: *SAE Tech. Pap.* (2012).
- [91] Rickard Solsjö. “Large Eddy Simulation of Turbulent Combustion in PPC and Diesel Engines”. In: *Ph.D Thesis, Lund Univ.* (2014).
- [92] Tommaso Lucchini et al. “Automatic Mech Generation for Full-Cycle CFD Modeling of IC Engines : Application to the TCC Test Case”. In: *SAE Tech. Pap.* (2014).
- [93] Amin Maghbouli et al. “Effects of grid alignment on modeling the spray and mixing process in direct injection diesel engines under non-reacting operating conditions”. In: *Appl. Therm. Eng.* 91.Complete (2015), pp. 901–912.
- [94] Yuanjiang Pei et al. “Large eddy simulation of a reacting spray flame with multiple realizations under compression ignition engine conditions”. In: *Combust. Flame* 162.12 (2015), pp. 4442–4455.
- [95] Christian Ibrón, Mehdi Jangi, and Xue-Song Bai. “Effects of In-Cylinder Flow Simplifications on Turbulent Mixing at Varying Injection Timings in a Piston Bowl PPC Engine”. In: *SAE Tech. Pap. Ser.* Vol. 1. 2019.

- [96] G. Woschni. "A universally applicable equation for the instantaneous heat transfer coefficient in the internal combustion engine". In: *SAE Tech. Pap.* 1967.
- [97] F. Berni et al. "Critical aspects on the use of thermal wall functions in CFD in-cylinder simulations of spark-ignition engines". In: *SAE Int. J. Commer. Veh.* 10.2 (2017).
- [98] S. Broekaert et al. "Experimental Investigation and Modelling of the In-Cylinder Heat Transfer during Ringing Combustion in an HCCI Engine". In: *SAE Tech. Pap.* 2017-March.March (2017).
- [99] Giuseppe Cicalese et al. "A Comprehensive CFD-CHT Methodology for the Characterization of a Diesel Engine: from the Heat Transfer Prediction to the Thermal Field Evaluation". In: *SAE Tech. Pap.* 2017-01-2196 (2017).
- [100] Helgi Skuli Fridriksson. "On CFD-Analysis of Heat Transfer of a Heavy-Duty Diesel Engine". In: (2011).
- [101] Helgi Fridriksson et al. "CFD Investigation of Heat Transfer in a Diesel Engine with Diesel and PPC Combustion Modes". In: *SAE Tech. Pap.* 2011-01-18 (2011).
- [102] Eric Gingrich, Jaal Ghandhi, and Rolf D. Reitz. "Experimental Investigation of Piston Heat Transfer in a Light Duty Engine Under Conventional Diesel, Homogeneous Charge Compression Ignition, and Reactivity Controlled Compression Ignition Combustion Regimes". In: *SAE Int. J. Engines* 7.1 (2014), pp. 2014–01–1182.
- [103] Christian Hennes, Jürgen Lehmann, and Thomas Koch. "Possibilities of Wall Heat Transfer Measurements at a Supercharged Euro VI Heavy-Duty Diesel Engine with High EGR-Rates, an In-Cylinder Peak Pressure of 250 Bar and an Injection Pressure up to 2500 Bar". In: *SAE Tech. Pap. Ser.* Vol. 1. 2019.
- [104] Christian Binder et al. "Heat Loss Analysis of a Steel Piston and a YSZ Coated Piston in a Heavy-Duty Diesel Engine Using Phosphor Thermometry Measurements". In: *SAE Int. J. Engines* 10.4 (2017), pp. 2017–01–1046.
- [105] Christian Binder et al. "Experimental Determination of the Heat Transfer Coefficient in Piston Cooling Galleries". In: *SAE Tech. Pap.* Vol. 2018-Sept. 2018.
- [106] Christian Binder et al. "Study on heat losses during flame impingement in a diesel engine using phosphor thermometry surface temperature measurements". In: *SAE Tech. Pap.* Vol. 2019-April. April. 2019.
- [107] Xin Yu et al. "Simulation and Experimental Measurement of CO₂^{*}, OH^{*} and CH₂O^{*} Chemiluminescence from an Optical Diesel Engine Fueled with n-Heptane". In: *SAE Tech. Pap. Ser.* 1 (2013).
- [108] Sara Lönn. "Investigation of PPC in an Optical Engine : With focus on Fuel Distribution and Combustion Characterization". PhD thesis. Lund University, 2019.

- [109] Scott A. Skeen, Julien Manin, and Lyle M. Pickett. “Simultaneous formaldehyde PLIF and high-speed schlieren imaging for ignition visualization in high-pressure spray flames”. In: *Proc. Combust. Inst.* 35.3 (2015), pp. 3167–3174.
- [110] Scott Skeen, Julien Manin, and Lyle M Pickett. “Visualization of Ignition Processes in High-Pressure Sprays with Multiple Injections of n-Dodecane”. In: *SAE Int. J. Engines* 8.2 (2015), pp. 696–715.
- [111] Scott A. Skeen et al. “A Progress Review on Soot Experiments and Modeling in the Engine Combustion Network (ECN)”. In: *SAE Int. J. Engines* 9.2 (2016).
- [112] Scott Skeen et al. “Standardized Optical Constants for Soot Quantification in High-Pressure Sprays”. In: *SAE Int. J. Engines* 11.6 (2018), pp. 805–816.
- [113] Ted Lind et al. “Simultaneous PLIF Imaging of OH and PLII Imaging of Soot for Studying the Late-Cycle Soot Oxidation in an Optical Heavy-Duty Diesel Engine”. In: *SAE Int. J. Engines* 9.2 (2016), pp. 849–858.
- [114] Ted Lind et al. “Mechanisms of Post-Injection Soot-Reduction Revealed by Visible and Diffused Back-Illumination Soot Extinction Imaging”. In: *SAE Tech. Pap.* Vol. 2018-April. 2018.
- [115] Zheming Li et al. “Comparison of Laser-Extinction and Natural Luminosity Measurements for Soot Probing in Diesel Optical Engines”. In: *SAE Tech. Pap.* Vol. 2016-October. 2016.
- [116] Christian Ibrón et al. “Large Eddy Simulation of an Ignition Front in a Heavy Duty Partially Premixed Combustion Engine”. In: *SAE Tech. Pap. Ser.* Vol. 1. SAE International, 2019.
- [117] Caroline L. Genzale, Rolf D. Reitz, and Mark P.B. Musculus. “Optical diagnostics and multi-dimensional modeling of spray targeting effects in late-injection low-temperature diesel combustion”. In: *SAE Int. J. Engines* 2.2 (2010), pp. 150–172.
- [118] Kan Zha et al. “A Study of Piston Geometry Effects on Late-Stage Combustion in a Light-Duty Optical Diesel Engine Using Combustion Image Velocimetry”. In: *SAE Int. J. Engines* 11.6 (2018), pp. 783–804.
- [119] Federico Perini et al. “Piston Bowl Geometry Effects on Combustion Development in a High-Speed Light-Duty Diesel Engine”. In: *SAE Tech. Pap. Ser.* Vol. 1. 2019.
- [120] Helgi Skuli Fridriksson et al. “CFD investigation on injection strategy and gasoline quality impact on in-cylinder temperature distribution and heat transfer in PPC”. In: *SAE Tech. Pap.* 6 (2013), p. 13.
- [121] Charles K. Westbrook and Frederick L. Dryer. “Comprehensive Mechanism for Methanol Oxidation”. In: *Combust. Sci. Technol.* 20.3-4 (1979), pp. 125–140.
- [122] C.-W. Zhou et al. “A comprehensive experimental and modeling study of isobutene oxidation”. In: *Combust. Flame* 167 (2015), pp. 353–379.

- [123] Ultan Burke et al. “A detailed chemical kinetic modeling, ignition delay time and jet-stirred reactor study of methanol oxidation”. In: *Combust. Flame* 165 (2016), pp. 125–136.
- [124] Wayne K. Metcalfe et al. “A hierarchical and comparative kinetic modeling study of C1- C2hydrocarbon and oxygenated fuels”. In: *Int. J. Chem. Kinet.* 45.10 (2013), pp. 638–675.
- [125] Moah Christensen and Alexander A. Konnov. “Laminar burning velocity of diacetyl + air flames. Further assessment of combustion chemistry of ketene”. In: *Combust. Flame* 178 (2017), pp. 97–110.
- [126] Gianluca Capriolo, Vladimir A. Alekseev, and Alexander A. Konnov. “An experimental and kinetic study of propanal oxidation”. In: *Combust. Flame* 197 (2018), pp. 11–21.
- [127] Stephen J. Klippenstein et al. “Uncertainty driven theoretical kinetics studies for CH₃OH ignition: HO₂ + CH₃OH and O₂ + CH₃OH”. In: *Proc. Combust. Inst.* 33.1 (2011), pp. 351–357.
- [128] Siyuan Hu, Cheng Gong, and Xue Song Bai. “Dual Fuel Combustion of N-heptane-methanol-air-EGR Mixtures”. In: *Energy Procedia* 105 (2017), pp. 4943–4948.
- [129] Kuichun Li et al. “Characteristics of Diesel Spray Flame under Flat Wall Impinging Condition –LAS, OH* Chemiluminescence and Two Color Pyrometry Results”. In: *SAE Tech. Pap. Ser. 1* (2014).
- [130] Kuichun Li et al. *Effect of Spray/Wall Interaction on Diesel Combustion and Soot Formation in Two-Dimensional Piston Cavity*. Tech. rep. 2013.
- [131] J. E. Rehm and P. H. Paul. “Reaction rate imaging”. In: *Proc. Combust. Inst.* 28.2 (2000), pp. 1775–1782.
- [132] Jonathan H. Frank, Sebastian A. Kaiser, and Marshall B. Long. “Reaction-rate, mixture-fraction, and temperature imaging in turbulent methane/air jet flames”. In: *Proc. Combust. Inst.* 29.2 (2002), pp. 2687–2694.
- [133] J. H. Frank, S. A. Kaiser, and M. B. Long. “Multiscalar imaging in partially premixed jet flames with argon dilution”. In: *Combust. Flame* 143.4 (2005), pp. 507–523.
- [134] Kar Mun Pang et al. “Investigation of chemical kinetics on soot formation event of n-Heptane spray combustion”. In: *SAE Tech. Pap.* 1.x (2014).

Summary of publications

Paper I: Effect of Start of Injection on the Combustion Characteristics in a Heavy-Duty DICI Engine Running on Methanol

M. Pucilowski, Mehdi Jangi, Sam Shamun, Changle Li, Martin Tunér, Xue-Song Bai
SAE Technical Paper 2017-01-0560, 2017

This paper presents numerical sweep of start of injection (SOI) to study mixing and combustion characteristics of methanol, which is based on a metal engine experiments with compression ratio 15:1. It is presented that due to the methanol fast mixing properties and cooling effect, the majority of the heat release rate is in the premixed combustion mode, even at SOI -3 CAD aTDC. The ignition sequence and the mixture composition for different injection strategies is studied in the $\phi - T$ diagram.

This work was conducted with collaboration with Division of Combustion Engines. The experimental data was generated and shared by Sam Shamun and Changle Li, supervised by Martin Tuner. The candidate performed all simulations and post-processing under supervision of Mehdi Jangi and Xue-Song Bai.

Paper II: Effect of Injection Pressure on the NO_x Emission Rates in a Heavy-Duty DICI Engine Running on Methanol

M. Pucilowski, Mehdi Jangi, Sam Shamun, Martin Tunér, Xue-Song Bai
SAE Technical Paper 2017-01-2194, 2017

This paper presents numerical study for the effect of injection pressure on the NO_x emissions based on the metal engine experiments with a high compression ratio of 27:1. It was found that by increasing injection pressure, the mode of combustion switched from the diffusion flame mode to the premixed combustion mode. The consequence was a large amount of premixed composition near the stoichiometric conditions that caused a higher average combustion temperature, and thus an increment of NO_x emissions.

This work was conducted with collaboration with Division of Combustion Engines. The ex-

perimental data was generated and shared by Sam Shamun, supervised by Martin Tuner. The candidate performed all simulations and post-processing under supervision of Mehdi Jangi and Xue-Song Bai.

Paper III: Heat Loss Analysis for Various Piston Geometries in a Heavy-Duty Methanol PPC Engine

M. Pucilowski, Mehdi Jangi, Sam Shamun, Martin Tunér, Xue-Song Bai
SAE Technical Paper 2018-01-1726, 2018

This paper presents a numerical study for heat transfer losses for various piston geometries in a methanol PPC engine with compression ratio 15:1. The goal was to identify the influence of each term in the wall heat transfer equation which are: the temperature gradient, the thermal conductivity, the piston area, and additionally exposure time, on the total wall heat losses. A reference case is methanol SOI -3 CAD aTDC at 5.42 bar IMEP_g under PPC conditions. The main mechanism behind the wall heat losses is the bulk flow, which governs the distribution of the hot combustion products. The stepped piston design, typical for the diesel engines, had the best properties of re-directing the hot combustion products away from the piston walls, which resulted in a lower wall heat losses.

This work was conducted with collaboration with Division of Combustion Engines. The experimental data was generated and shared by Sam Shamun, supervised by Martin Tuner. The candidate performed all simulations and post-processing under supervision of Mehdi Jangi and Xue-Song Bai.

Paper IV: Comparison of Kinetic Mechanisms for Numerical Simulation of Methanol Combustion in DICI Heavy-Duty Engine

M. Pucilowski, Rui Li, Shijie Xu, Changle Li, Fei Qin Martin Tunér, Xue-Song Bai, Alexander A. Konnov
SAE Technical Paper 2018-01-0208, 2018

This paper presents a literature survey and performance comparison for methanol chemical kinetic models based on the state-of-the-art experiments and high fidelity 0-D, 1-D and 3-D numerical simulations. It is showed that performance of skeleton mechanisms is in good agreement with performance of their detailed versions.

This work was conducted with collaboration with Division of Combustion Engines and Division of Combustion Physics. The engine experimental data was generated and shared by Changle Li, supervised by Martin Tuner. The methanol kinetic mechanisms were prepared by Rui Li under supervision of Fei Qin and Alexander A. Konnov. Shijie Xu helped to translate mechanisms to OpenFOAM version. Rui Li also performed 0-D and 1-D simulations. The candidate performed

all 3-D engine simulations and coordinated article writing process based on the contributions from the co-authors under supervision of Xue-Song Bai.

Paper V: Numerical Investigation of Methanol Ignition Sequence in an Optical PPC Engine with Multiply Injection Strategies

M. Pucilowski, Hesameddin Fatehi, Mehdi Jangi, Sara Lönn, Alexios Matamis, Övind Andersson, Mattias Richter, Xue-Song Bai

14th international Conference on Engines & Vehicles, 19ICENA-0262, 2019

This paper presents a numerical study of ignition sequence of methanol in an optical engine setup with compression ratio of 16:1. The goal is to validate the fuel injection process and the onset of ignition based on the optical data. Combustion mode analysis was performed based on the distribution of the heat release rate and the key species as fuel, oxygen and carbon monoxide. Both injection strategies resulted in the fuel lean and the fuel rich mixtures, which led to combination of premixed and non-premixed burn, i.e., PPC.

This work was conducted with collaboration with Division of Combustion Engines and Division of Combustion Physics. The experimental data was generated and shared by Sara Lönn and Alexios Matamis, supervised by Övind Andersson and Mattias Richter. The candidate performed all numerical simulations and post-processing under supervision of Mehdi Jangi and Xue-Song Bai. The article was written together with Hesameddin Fatehi.

Paper VI: LES study of diesel spray/wall interaction and mixing mechanisms at different wall distances

M. Pucilowski, Mehdi Jangi, Hesameddin Fatehi, Kar Mun Pang, Xue-Song Bai
Preprint submitted to Proceedings of the Combustion Institute

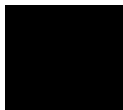
This paper presents a numerical study for diesel spray - wall interaction at various wall positions based on experimental findings in the constant volume vessel. The goal was to understand the change of mixing mechanisms as the lift-off length, impingement mixing and entrainment wave mixing, due to the wall interaction. It was found that wall jet configurations (30 mm and 50 mm distance between the wall and nozzle) have a higher air entrainment rate after the end of injection, which was the reason behind a faster oxidation of soot emissions compared to the free jet case.

The candidate performed all numerical simulations and post-processing. Kar Mun Pang assisted in a number of test simulations and participated in discussions. The article was written by the candidate under supervision of Mehdi Jangi, Hesameddin Fatehi, and Xue-Song Bai.

Paper I



Paper II



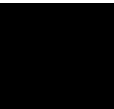
Paper III



Paper IV



Paper V



Paper VI



